ARMY RESEARCH LABORATORY

Electron-Beam (E-Beam) Processing as a Means of Achieving High Performance Composite Structures

by James M. Sands, Steven H. McKnight, Bruce K. Fink, Anna Yen, and Giuseppe R. Palmese

ARL-TR-2613 November 2001

The findings in this report are not to be construed as an official Department of the Army position unless so designated by other authorized documents.

Citation of manufacturer's or trade names does not constitute an official endorsement or approval of the use thereof.

Destroy this report when it is no longer needed. Do not return it to the originator.

Army Research Laboratory
Aberdeen Proving Ground, MD 21005-5069

ARL-TR-2613 **November 2001**

Electron-Beam (E-Beam) Processing as a Means of Achieving High Performance Composite Structures

James M. Sands, Steven H. McKnight, and Bruce K. Fink
Weapons and Materials Research Directorate, ARL

Anna Yen
Northrop Grumman Corporation

Giuseppe R. Palmese
Drexel University

Abstract

Electron-beam (E-beam) curing is among the key out-of-autoclave technologies being explored for future advanced composite and adhesive applications. E-beam irradiation curing is capable of rapid and through-thickness curing of composite samples up to 2-in thickness, eliminating the need for long cure cycles in the autoclave. However, current resin and adhesive chemistries are optimized for cure by thermal initiation, which involves slow ramps and long cure cycles, particularly for thermoset composites based on epoxides. Therefore, in order to provide improved performance in composite systems cured by E-beam irradiation, a program was undertaken to investigate performance and formulation effects in two E-beam curable systems. One system, a free-radical-cured acrylic system, introduces the concept of interpentrating network structures as a means of meeting performance requirements in E-beam-processed composites. The second resin system incorporates cationic curing of epoxides induced through Lewis acid or cation generating initiators. Additionally, a new approach to toughened interpenetrating polymer networks (IPNs) based on simultaneous cure using both free-radical and cationic-cure mechanisms is proposed along with initial experimental characterizations. The results of formulation and processing modifications on key properties of adhesives, resins, and composites structures are demonstrated.

Acknowledgments

We gratefully acknowledge the Shell Chemical Company and Air Products for providing material samples during the testing and formulation phase of this project. Additionally, support for this work was provided by the U.S. Department of Defense through the Strategic Environmental Research and Development Program (SERDP).

INTENTIONALLY LEFT BLANK.

Contents

List of Figures

List of Tables

INTENTIONALLY LEFT BLANK.

1. Introduction

The electron-beam (E-beam) accelerator is a source of ionizing radiation that can generate ionic species, free radicals, and molecules in excited states capable of initiating and sustaining polymerization. Depending on the chemistry of the resin system being irradiated, polymerization can occur by free radical as well as ionic mechanisms. The polymerization of acrylate systems, maleic and fumaric polyester resins, and thiol-ene systems proceeds by free-radical propagation without initiators because radicals are induced in large number in the unsaturated resin. Non-radical curing occurs in other monomer systems. For instance, E-beam-induced polymerization of nitroethylene proceeds via anionic mechanisms, while epoxides polymerize via cationic propagation with the appropriate catalyst. Of these systems, free-radical-cured systems based on methacrylate functionality and cationically cured epoxides catalyzed using diaryliodonium or triarylsulfonium salts, like diphenyliodium hexalfluoroantimonate (DPI) or triarylsulfonium hexalfluoroantimonate (TAS), have shown the most promise for composites applications.

Methacrylate-based free-radical-cured systems can be initiated using either a catalyst and thermal cure or without catalyst using ionizing radiation. E-beam-cured methacrylate polymer thermosets achieve a high degree of monomer conversion, possess high stiffness, contain adjustable processing viscosities, and have a very long shelf life. However, among the shortcomings historically associated with such systems are high cure shrinkage (8–20%), the potential for oxygen inhibition, and lower glass transition temperature (T_g) relative to high-temperature thermally cured epoxies. The high degree of shrinkage on cure typically results in residual stresses in the resin on cooling, which produces brittle matrix materials, and often results in preload fracture of glass or carbon fibers or component warpage in composite applications. In addition, acrylic materials have a low ceiling temperature where the polymer reverts to monomers at high temperatures in the presence of oxygen, resulting in off-gassing of hazardous monomer fumes during combustion.

One approach to decreasing cure shrinkage is to modify the chemistry using blends of low-shrinkage monomers in addition to traditional methacrylate matrix materials. The attempt to reduce shrinkage and increase compatibility between resin and composite fabrics included development of an interpenetrating polymer network (IPN) based on epoxides and compatible acrylate monomer blends [1]. The success of the IPN approach to providing improved composite performance has led to increased investigations into compatible matrix formulations based on IPN constructs [2]. IPNs are cured according to a number of different approaches using thermal and E-beam

irraditiation to achieve high conversion of matrix in thick-section (up to 2-in) composite laminates. The recent developments on methacrylate and epoxide IPNs based on digycidyl ether of bis-phenol A (DGEBA) backbone structures are now used to prepare composite and adhesive systems including vacuum-assisted resin-transfer molding (VARTM) processable resins, paste and film adhesives, and composite carbon-fiber prepregs.

Cationically cured epoxies require a photoinitiator to enable polymerization but offer lower shrinkage, exhibit higher T_g, and are not inhibited by oxygen. On the other hand, cationic systems tend to cure more slowly than free-radical systems, and the photoinitiators are easily poisoned by nucleophilic contaminants, which are often found on the surfaces of reinforcing materials or as part of epoxy resin compositions. In addition, aging of the resin becomes an issue because exposure to ambient light can induce an excited state in the catalyst and slow curing of the resins, thereby changing cure cycle characteristics important for manufacturing.

A new approach to E-beam-only cured composite structures has recently been initiated using the formulating variety of IPN chemistry to achieve improved toughness for cationic cured epoxides. The combination of cationic-cured epoxides and free-radical-cured methacrylates simultaneously cured has produced unique dynamic mechanical results for these latest polymer systems. Because the cure mechanisms for cationic and free-radical systems are independent, these two networks when combined in an optimized concentration result in highly converted networks with excellent potential to provide toughness to the two brittle matrix systems with IPN design [3, 4].

In this report, all of the previously mentioned approaches are investigated and reported at various levels of completion. The work addresses a complete set of resin forms for composite repair of aerospace and ground vehicle structures. Therefore, we evaluate processing and formulation approaches for VARTM, adhesive, prepreg methods of composite manufacture. Our cure cycles cover the range of room-temperature or low-temperature thermal staging followed by E-beam cure to solely E-beam cured systems. Our results demonstrate the high potential for improving E-beam resin performances using a wide range of approaches to increasing toughness of the matrix resin used in composite manufacturing.

2. Technology Developments in E-Beam Cure

2.1 Toughened E-Beam Resins for VARTM

VARTM has become an important low-cost composite processing technique. VARTM processing combined with E-beam curing can offer advantages such as

reduced energy consumption, curing at selectable temperature, and higher degree of monomer conversion over the traditional thermal curing process. Radiation can initiate free-radical or ionic polymerization. In this program, we developed a new generation of radiation-cured systems based on free-radical curing. This novel system uses IPN synthesis as discussed in earlier reports [3–5] A second-tier effort involved investigation of the cationic cure technology.

The curing process of an epoxy-vinyl-based IPN system (shown schematically in Figure 1) involves step-growth as well as free-radical polymerization. The step-growth reaction takes place between epoxy and amine, while free-radical curing brings about polymerization of vinyl-containing monomers. The resin is a mixture of difunctional epoxy, tetra-functional amine, a unique bifunctional monomer possessing epoxy and vinyl functionality, and divinyl monomers. The resin mixture is cured initially at low temperature, where the epoxy-amine forms a polymer network while the vinyl monomer remains unreacted inside the network. The epoxy end of the bifunctional monomer becomes a part of the epoxy-amine network upon initial thermal curing, while the vinyl end remains pendant on the network. This constitutes a C-stage structure. The C-stage material is then cured completely by E-beam to form a second network from vinyl monomers. The polymerization of pendant vinyl groups along with the diluents provides co-continuity between the two networks. The combination of two networks forms an IPN. Since the two polymer networks were formed sequentially, the two-stage cure approach produces two independent networks of compatible polymer thermosets and is called a "sequential IPN."

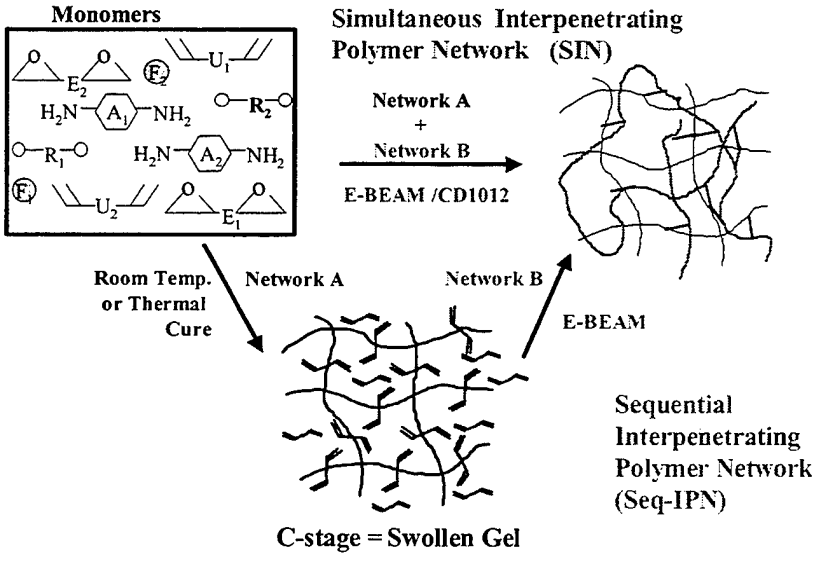

Figure 1. IPN processing for E-beam curable resins.

In addition to toughening achieved by IPN formulation, traditional approaches to toughening including chain extension, or increase of chain length between crosslinks, and thermoplastic or rubber toughening are applied to these IPN systems. Because the two networks are cured from monomer compatible resins, our early investigations of these systems included mapping of the phase diagram of rubber-toughened systems to determine an optimum window for formulations to remain single-phase. An optimum toughened system will produce phase-separated structures after thermal staging (C-staging). The phase development of epoxy-terminated butyl nitrile (ETBN) rubbers has been reported [3, 4, 6]. The use of thermal staging allows the formulator to achieve slow-developing phase separation of rubber for improved toughness. We extend this approach to other toughening agents, including dendrimers and thermoplastic oligomers in additional resin systems, to achieve low-viscosity resins for VARTM processing.

Using the IPN formulation concept, we developed base E-beam-curable resin systems with low (250 °F) and high T_g. These resins are prepared using DGEBA monomers as the backbone for both the epoxide and methacrylate thermoset polymers. The method of increasing T_g usually involves increasing the crosslink density or decreasing the distance between crosslinks by adding higher functional monomers (f>3) to the matrix formulation. However, this approach has a deliterious impact on fracture behavior. Therefore, the T_g is used as one parameter to separate systems for fracture comparisons. Formerly, we explored achieving better performance of the 250 °F T_g resin systems via manipulation of the initial epoxy-amine network, increasing flexibility of the network and adding toughening agents. The results of the 250 °F T_g developments for VARTM composites are shown in Table 1. For 350 °F T_g systems, the use of toughening agents chemically incorporated into the second network of an IPN was also investigated. The overall goal was to obtain VARTM resin systems that meet a processing requirement of viscosity less than 500 centipoise (cP) at room temperature and also possess a good balance of mechanical properties including modulus, strength, and fracture toughness.

Formulation work has continued to address improvements in the performance of these resin systems by increasing fracture toughness while reducing viscosity. This has proven to be particularly successful regarding 250 °F resin systems. We demonstrated that dendritic polymers (E1) can be used to reduce viscosity and increase fracture toughness, as demonstrated by VCCMD.1 in Table 1. However, for dendritic-based resins, toughness as measured by G_{IC} was found to be significantly lower (370 J/m^2) than that for analogous materials toughened using ETBN (500 J/m^2). Moreover, a significant reduction of modulus and T_g was observed for dendrimer toughened systems.

Table 1. Properties of DGEBA-type VARTM resins for E-beam processing.

Resin Description	VCCM1.1 250 °F	VCCM4.1 Toughened 250 °F	VCCMD.1 Toughened 250 °F	VCCMU3.1 350 °F
T_g (°C)[a]	132	129	119	172
Wet T_g (°C)[a, b]	113	110	NA	153
Viscosity (cP) RT	290	470	370	395
Viscosity w/curing agent (cP) RT	~240	~320	280	~280
Flexural modulus (ksi)[c]	530 ± 25	560 ± 35	NA	550 ± 35
Flexural strength (ksi)[c]	18.4 ± 0.8	18.6 ± 1.0	NA	16.0 ± 0.7
K_{IC} (MPam$^{0.5}$)[d]	1.2 ± 0.05	1.5 ± 0.1	1.2 ± 0.05	0.8 ± 0.05
E' (GPa)	3.0	2.5	2.3	NA
G_{IC} (J/m^2)[d]	250 ± 30	500 ± 40	370 ± 40	180 ± 25

Note: C-staging: 50 °C for 5 hr or 2 hr at 50 °C + 1 hr at 70 °C.

Note: E-beam: 20 Mrad (passes of 2 × 0.5 Mrad/2 × 2 Mrad/3 × 5 Mrad).

[a]Tg from dynamic mechanical analysis (DMA) (5 °C/min to 200 °C) E" peak-second run.

[b]48-hr water boil.

[c]ASTM D790-96a [7].

[d]ASTM D5045-93 [8].

A new series of 250 °F resins based on a lower viscosity dimethacrylate derived from diglcidyl ether of bisphenol F (DGEBF) rather than DGEBA was evaluated. This set of resins (series 6) also uses new combinations of toughening agents that show significantly improved toughness over previous systems. The base resin VCCM1.6 was modified using the dendritic and reactive additives employed in the DGEBA systems. Formulation modifications are shown in encoded form in Table 2.

Table 2. Composition of series-6, DGEBF-type 250 °F resins.

Set	Base resin	Toughener
VCCM1.6	CCM1	Untoughened baseline
VCCM4.6	VCCM1.6	R1 (5%)
VCCMD.6	VCCM1.6	E1 (10%)
VCCMD.6b	VCCM1.6	E1 (5%)
VCCM4D.6	VCCM1.2	R1 (5%) + E1 (5%)

The results of resin testing for series 6 resins are summarized in Table 3. Generally, these resins compare favorably with the DGEBA-based 250 °F resins. For example, the mechanical characteristics of VCCM1.1, VCCM4.1, and VCCMD.1 are similar to those obtained for the analogs VCCM1.6, VCCM4.6, and VCCMD.6, yet the later set is less viscous. Additionally, experiences with high concentrations of E1 (>7%) resulted in excessive phase separation that reduced strength considerably. Reducing the content of E1 dendrimer from 10% to 5% actually produced higher fracture toughness in the IPNs, despite conventional wisdom and formulation guides for the E1 that suggest 10% for optimum

Table 3. Properties of series-6, DGEBF-type 250 °F resins.

Resin	E'' peak T_g (°C)	G_{IC} (J/m²)	K_{IC} (MPa.m$^{0.5}$)	E' (Gpa)	Viscosity (cP)
VCCM1.6	130	264 ± 87	1.2 ± 0.05	2.9	210
VCCM4.6	125	506 ± 70	1.4 ± 0.05	2.7	400
VCCMD.6	110	395 ± 120	1.2 ± 0.05	2.5	320
VCCMDb.6	115	497 ± 120	1.3 ± 0.05	2.6	<370
VCCM4D.6	115	850 ± 140	1.8 ± 0.05	2.7	360

toughness. We can attribute this small difference in concentration to the different chemical environment of the IPNs compared to traditional epoxides. More dramatic was the effect of combining tougheners as shown by VCCM4D.6 that uses both the ETBN and E1 second phase additives. This system has a G_{IC} that is 60% greater than VCCM4.1 and viscosity that is at least 25% lower. The modulus remains high. However, the dendritic component appears to reduce T_g (T_g < 115 °C) significantly in all of the sample formulations in which it appears. Plots showing the storage and loss modulus as a function of temperature are given in Figure 2. These exhibit good behavior similar to previously studied systems in Figure 3.

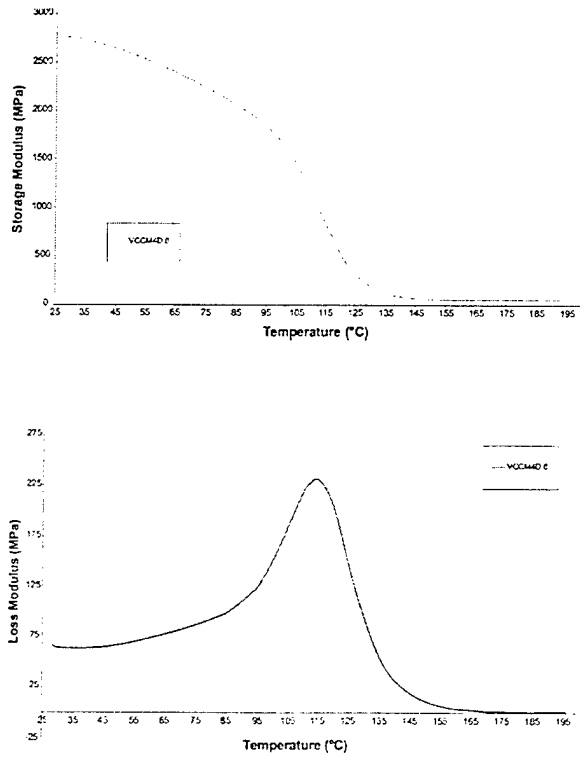

Figure 2. Storage (top) and loss modulus (bottom) obtained by DMA for E-beam-cured VCCM4D.6, a DGEBF-type toughened resin.

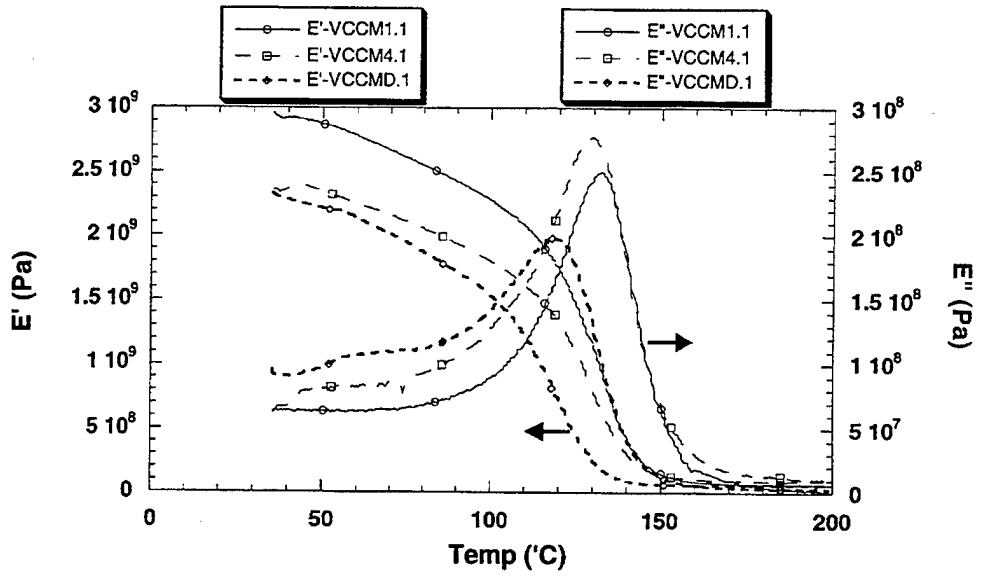

Figure 3. Storage (E') and loss (E") modulus as a function of temperature for post-cured DGEBA-type E-beam resins.

2.2 Adhesive Pastes

VARTM systems are a critical component of the manufacturing aspects associated with alternative processing of composite structures. However, an additional component—high performance adhesive systems—is required to achieve repair in most composite platforms. Therefore, we investigated developments of high performance adhesives resulting from IPN formulations and using a paste-type adhesive approach. The greatest difference between adhesive paste systems and VARTM resins is a high viscosity and low-sag resistance requirement on paste adhesives. The high viscosity of paste adhesives allows the use of toughening agents that would be difficult to incorporate in VARTM formulations. However, due to the great success of the VARTM developments, we also explored the effects of ETBN and dendrimers for toughening performance in adhesives. Previously, we reported the development of a novel IPN adhesive based on similar formulations to those used for VARTM composites [3]. Therefore, these paste adhesives involved a two-stage cure process including a low-temperature (~50 °C for 3 hr) staging followed by E-beam irradiation for methacrylate cure. The adhesive performance was tested on aluminum and composite substrates and demonstrated a twofold increase in adhesive performance over untoughened epoxy or IPN baselines. In addition, the hot/wet performance of the adhesives showed 80% retention of performance at 220 °F, which is a marked improvement over former systems available for E-beam adhesive applications.

A number of questions remained unclear after the development phase of E-beam adhesives, including the excellent performing ADEP01. Therefore, we

investigated the dynamic mechanical performance of the adhesive compounds and compared the IPN-type epoxy/methacrylate adhesives with traditional toughened epoxide adhesive formulas. In particular, we report here results from dynamic mechanical analysis (DMA) investigations of model IPN adhesives looking at the microstructural and macrostructural characteristics of the paste adhesives. DMA investigations were particularly employed to elucidate the variation in performance between E-beam-processed and thermally cured methacrylate networks in the IPN adhesives.

Based upon the ADEP01 formulation baseline, preliminary formulations were developed where the epoxide and methacrylate networks are mixed in approximately equal weight fractions (e.g., 50/50). Two compositions (with and without ETBN) and two cure methods (E-beam and thermal) were chosen to provide insight into the role of cure condition and elastomer modification on the structure and properties of the sequential IPNs (SeqIPNs). Additionally, the cure behavior and properties of the SeqIPNs are compared to model networks consisting of both ETBN-modified and unmodified epoxy-amine thermosets. These model systems are formulated without diluents and are traditional thermoset epoxy networks. The compositions of the systems described here are listed by weight-percent in Table 4.

Table 4. Chemical compositions of experimental and model resins (weight-percent).

System	Cure Type	Amine	DGEBA	ETBN	MDGEBA[a]	HDDMA[b]	BDGEBA[c]
I00E	E-beam	9.2	32.9	0	38.8	10	9.1
I01E	E-beam	8.5	30.4	9.7	32.1	10	7.7
I00T	Thermal	9.2	32.9	0	38.8	10	9.1
I01T	Thermal	8.5	30.4	9.7	32.1	10	7.7
E00T	Thermal	22.7	77.3	0	0	0	0
E01T	Thermal	20	70	10	0	0	0

[a]Methacrylated diglycidyl ether of bisphenol A.
[b]Hexanediol dimethacrylate.
[c]Bifunctional diglycidyl ether of bisphenol A.

DMA of multi-component interpenetrating networks is a proven method of characterizing the level of compatibility between the various network constituents [9–12]. Typically, highly miscible IPNs exhibit a single T_g, while phase-separated IPNs display two distinct glass transitions—one for each network. Figure 4 illustrates the dynamic E" curves for the thermally and E-beam-cured neat and rubber-toughened SeqIPN adhesives as well as the neat and rubber-toughened model epoxy for comparison. The addition of the rubber-toughener to the model epoxy-amine (EA) network results in a slight decrease in T_g, from 155 °C to 147 °C. The T_g was taken as the maximum temperature of the peak for the primary α transition. The shape of the secondary β relaxation for the rubber-toughened epoxy is also changed in comparison to the neat model EA network. The rubber-toughened model EA network displays a new transition at

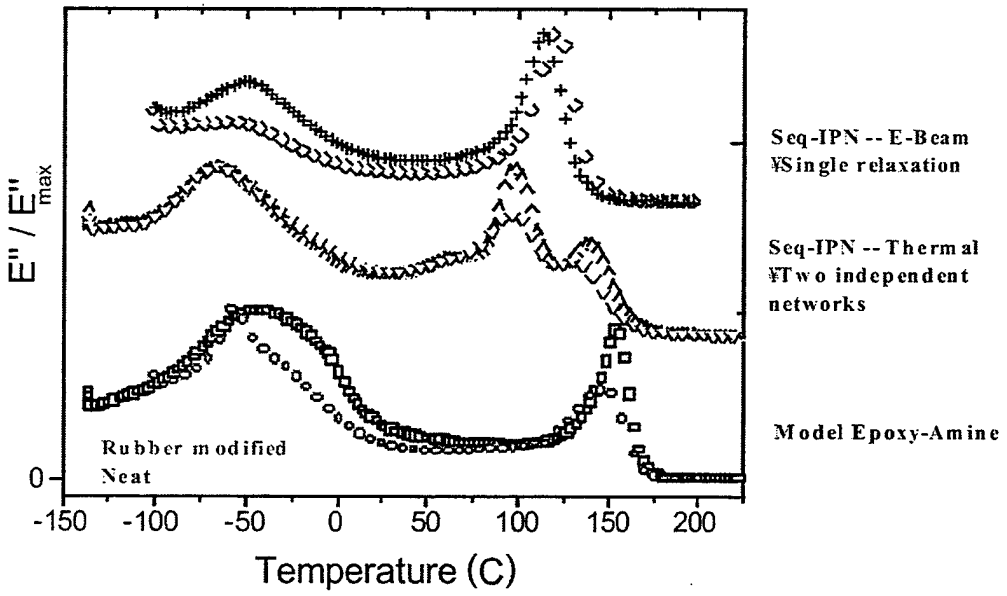

Figure 4. Normalized modulus for IPN-based paste adhesives cured by E-beam and thermal processing.

-56 °C, which is not evident in the broad secondary β relaxation of the neat EA network, and is ascribed to phase-separated rubber-rich domains. The E" spectra for the thermally cured SeqIPNs reveal the presence of two α-transition peaks for both the neat and rubber-toughened SeqIPN networks. The primary α transition (α_1 = 140 °C) is attributed to the glass transition of the EA network, while the secondary α transition (α_2 = 98 °C) is the glass transition of the methacrylate network. Upon addition of the ETBN rubber toughener, the T_g of the α_2 transition remains nearly unchanged at 96 °C. However, the T_g of the α_1 transition in the rubber-toughened SeqIPN has decreased slightly to 132 °C, which may be due to partial solubility of the elastomer in the EA phase. The slight decrease of T_g for the EA network upon addition of the ETBN is a good indication that the rubber toughener is experiencing some degree of phase separation in the cured SeqIPN network [13]. However, the evidence of an additional low temperature E" peak is absent in the 1-Hz DMA spectra of the rubber-toughened thermally cured SeqIPN. In contrast to the thermally cured SeqIPNs, the E-beam-curing method produces a single E" peak at the α transition. The T_g of the E-beam-cured SeqIPN is slightly reduced by the rubber toughener from 121 °C to 113 °C. The relative magnitude of the secondary β relaxation is greater for the rubber-toughened E-beam-cured SeqIPN when compared to the neat counterpart, but the shape of the relaxation peak is similar. The DMA and differential scanning calorimetry (DSC) results are summarized in Table 5.

Table 5. Thermal characterization results, WLF parameters, and KWW parameters.

System	T_g DSC (°C)	T_g DMA (°C)	C_1	C_2 (K)	β	τ^* (s)
I00E	107	121	15.1	77.6	0.218	0.053
I01E	110	113	15.7	76.7	0.210	0.11
I00T	119	$\alpha_1 = 140$ $\alpha_2 = 98$	–	–	–	–
I01T	110	$\alpha_1 = 132$ $\alpha_2 = 96$	–	–	–	–
E00T	160	155	15.3	74.3	0.203	0.035
E01T	151	147	17.6	73.0	0.168	0.17

A more thorough evaluation of these systems has been published in a recent journal article [6].

In addition to these characterization improvements, we also developed a series of improved peel versions of ADEP01 adhesive. The DMA investigations described here demonstrated that phase separation of these mixed epoxy/methacrylate IPNs is still not optimum, and therefore toughness is not optimized, despite our excellent performance. We therefore evaluated a number of additional toughening for phase separation and peel performance. The tougheners were used for both thermal and E-beam-processed adhesive formulations. The materials used included flexible monomers for co-curing in the methacrylate network, additional ETBN-diluent combinations, and dendrimers. Our screening showed that combinations of ETBN-diluents and dendrimer could provide increased peel performance, comparable to the results observed in VARTM resin systems.

2.3 VARTM Carbon Fiber Composites

Composite panels have been fabricated and tested using the VARTM process in combination with the IPN-based E-beam resin described previously. VCCM1.1, VCCM4.1 untoughened and toughened 250 °F resins and the 350 °F VCCMU3.1 untoughened system were evaluated. G'-sized AS4 5HS carbon fabric was used for the panels. The fabric areal weight was 370 g/m^2, and eight plies were used for each panel. Tables 6 and 7 report the properties for these composites following E-beam cure and following a post-cure cycle, respectively. The cure cycles for the composites are given in the tables. In addition, the property values are summarized in the same tables. Figures 5–8 are bar charts which facilitate comparison of properties. Figure 5 gives interlaminar shear strength results. Figures 6–8 provide summaries of tensile, flexural, and compressive strength normalized to 60% fiber volume fraction, respectively. The interlaminar shear strength, and to a lesser degree compressive strength, correlate with the fracture toughness of the resin systems. Thus, the composites based on VCCM4.1 have high interlaminar shear strength (8.7 ksi) compared with the very brittle high temperature VCCMU3.1 system (7.0 ksi). Unexpectedly, the tensile properties also appear to follow the same trend. Flexural strength is lowest for VCCMU3.1.

Table 6. Composite properties prior to post-curing (12k 5HS AS4 G').

Property	VCCM1.1	VCCM4.1	VCCMU3.1
Volume fraction (%)	60 ± 3	55 ± 2	56 ± 2
Void content (%)	<1	<1	<1
Tensile strength (ksi)[a]	117 ± 10	116 ± 8	111 ± 8
Tensile modulus[a]	10.3 ± 0.2	9.6 ± 0.7	9.7 ± 0.6
Compressive strength (ksi)[b]	95 ± 7	98 ± 5	93 ± 2
Compressive modulus (msi)[b]	9.7 ± 0.3	9.6 ± 0.1	9.1 ± 0.3
Iosipescu shear strength (ksi)[c]	12 ± 0.7	11.6 ± 0.4	11.5 ± 0.4
Iosipescu shear modulus (msi)[c]	0.65 ± 0.03	0.64 ± 0.04	0.64 ± 0.04
Flexural strength (ksi)[d]	128 ± 15	120 ± 11	114 ± 10
Flexural modulus (msi)[d]	10.1 ± 0.5	9.3 ± 0.1	9.1 ± 0.2
Short beam shear strength (ksi)	8.4 ± 0.2	8.8 ± 0.2	7.2 ± 0.2

Note: C-staging: 50 °C for 5 hr or 2 hr at 50 °C + 1 hr at 70 °C.
Note: E-beam: 20 Mrad (passes of 2 × 0.5 Mrad/2 × 2 Mrad/3 × 5 Mrad).
[a]ASTM D3039M-95a [14].
[b]ASTM D3410M-95 [15].
[c]ASTM D5379/D5379M-98 [16].
[d]ASTM D790-96a [7].

Table 7. Composite properties following post-curing (12k 5HS AS4 G').

Property	VCCM1	VCCM4	VCCMU3.1
Volume fraction (%)	60 ± 3	55 ± 2	56 ± 2
Void content (%)	<1	<1	<1
Tensile strength (ksi)[a]	134 ± 13	118 ± 6	105 ± 5
Tensile modulus[a]	9.9 ± 0.3	9.3 ± 0.1	9.0 ± 0.7
Compressive strength (ksi)[b]	84 ± 7	93 ± 3	74 ± 10
Compressive modulus (msi)[b]	9.8 ± 0.2	9.4 ± 0.4	8.8 ± 0.1
Flexural strength (ksi)[c]	136 ± 15	129 ± 4	121 ± 10
Flexural modulus (msi)[c]	10.5 ± 0.4	9.9 ± 0.5	10.2 ± 0.2
Short beam shear strength (ksi)	8.1 ± 0.4	8.0 ± 0.3	6.2 ± 0.5

Note: C-staging: 50 °C for 5 hr or 2 hr at 50 °C + 1 hr at 70 °C.
Note: E-beam: 20 Mrad (passes of 2 × 0.5 Mrad/2 × 2 Mrad/3 × 5 Mrad).
[a]ASTM D3039M-95a [14].
[b]ASTM D3410M-95 [15].
[c]ASTM D790-96 [7].

An interesting finding is that post-curing significantly alters composite properties. Generally, interlaminar shear and compressive strength are reduced by roughly 10-20%, with the greatest decrease occurring for the more brittle systems. On the other hand, tensile strength increases by roughly 10%, and little change is observed for flexural properties. It can be concluded that our efforts to toughen the IPN-based E-beam resins resulted in composites with significantly improved performance.

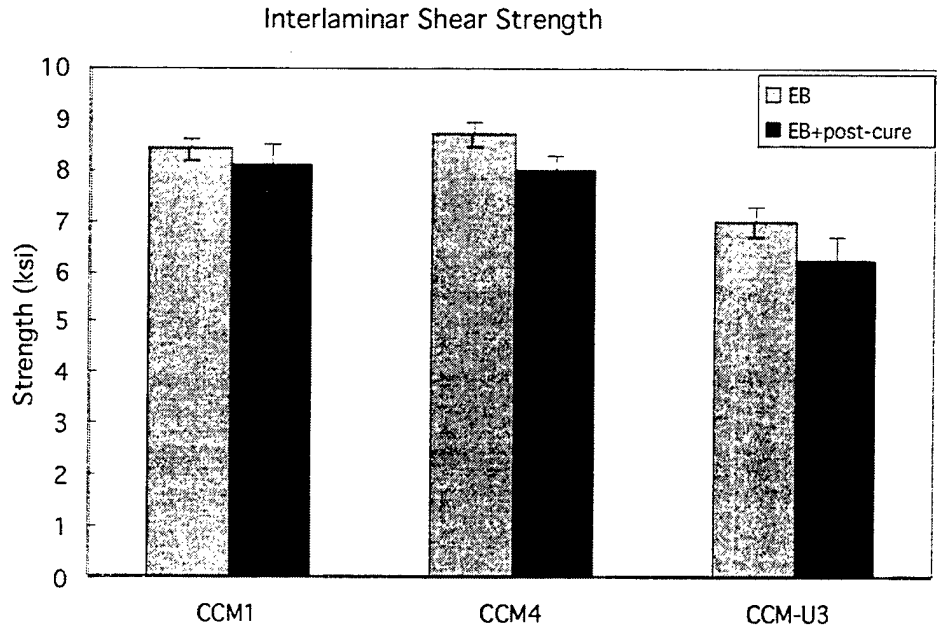

Figure 5. Interlaminar shear strength for E-beam and E-beam/post-cured systems.

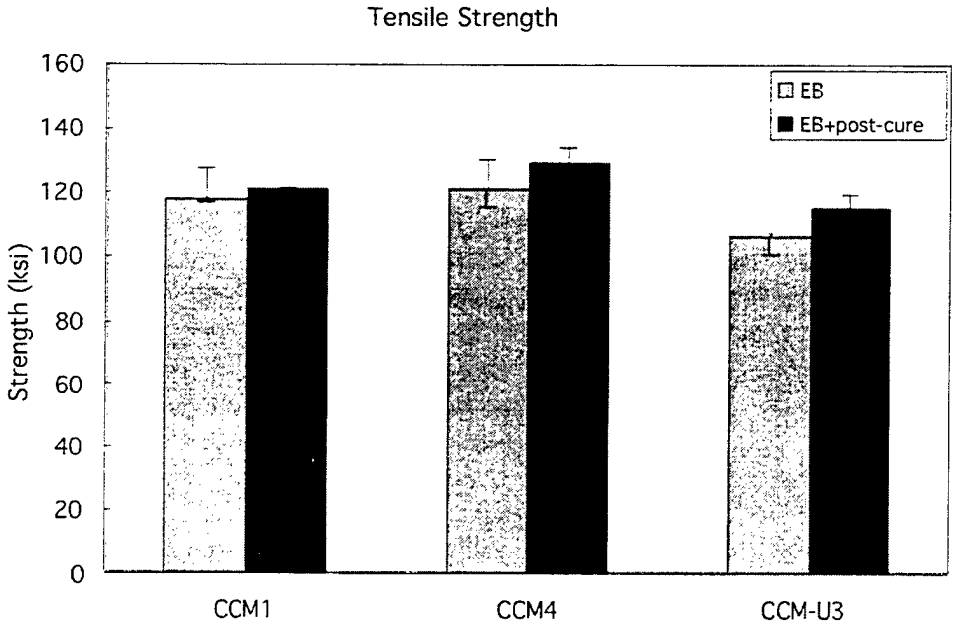

Figure 6. Tensile strength (60% fiber) for E-beam and E-beam/post-cured systems.

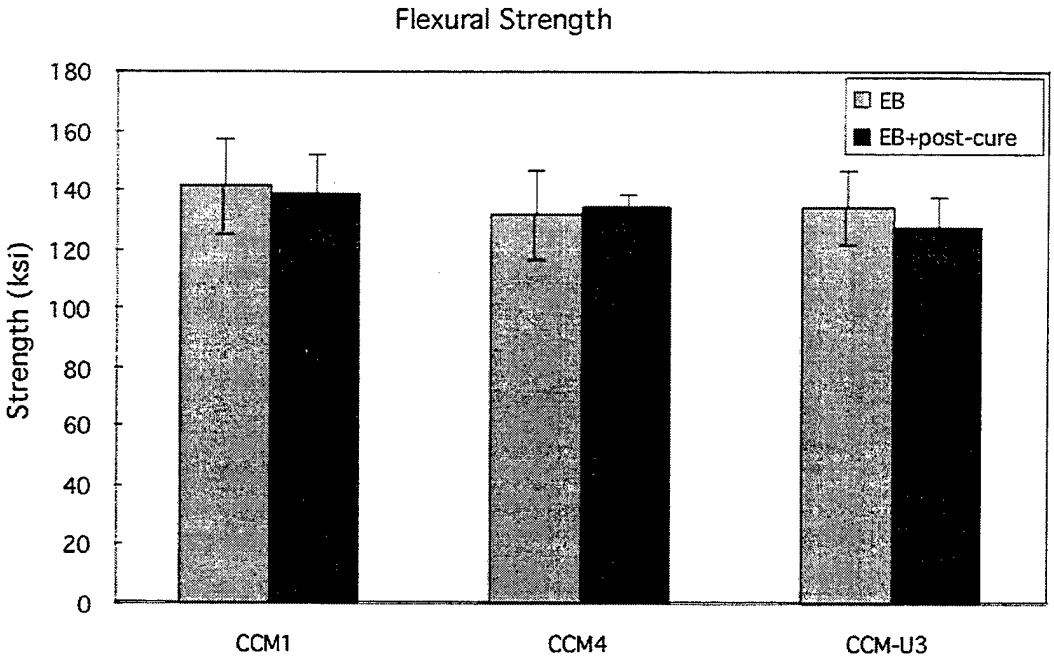

Figure 7. Flexural strength (60% fiber) for E-beam and E-beam/post-cured systems.

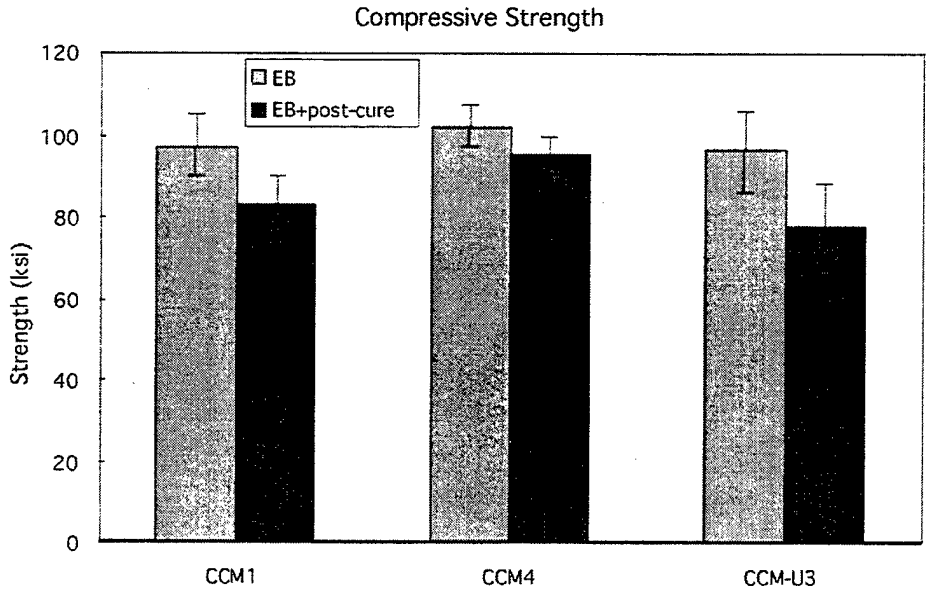

Figure 8. Compressive strength (60% fiber) for E-beam and E-beam/post-cured systems.

2.4 Mechanisms of Cure for E-Beam-Induced Cationic Cured Epoxies

The cationic homopolymerization of epoxy initiated by BF_3-amine catalysts is akin to E-beam-induced polymerization, and understanding the polymerization of such systems provides a basis for investigating E-beam-induced cationic cure of epoxies.

The salt $R'NH_3^+BF_4^-$ is thought to activate the epoxy monomer (M) by forming an oxonium ion active center (MH^+) as shown in equation 1:

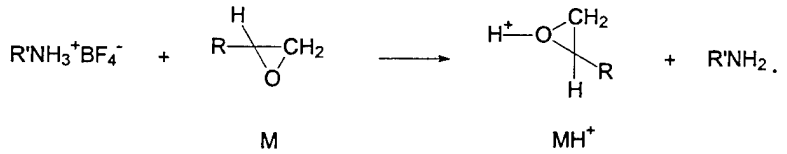

(1)

The propagation in such cationic polymerizations has been reported to proceed via two competing mechanisms known as the activated chain end (ACE) or activated monomer (AM) mechanism given in equations 2 and 3, respectively.

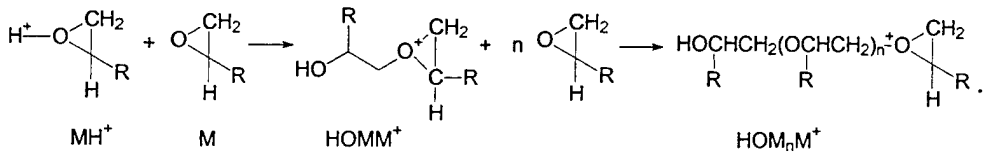

(2)

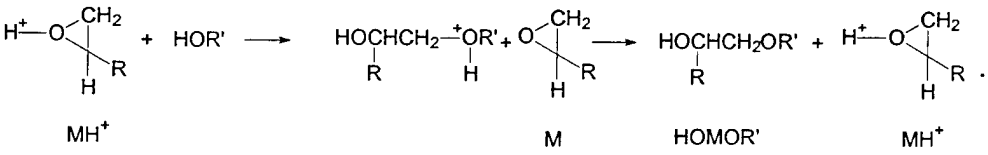

(3)

In the ACE mechanism, growing chain cyclic tertiary oxonium ions ($OHMM^+$) are formed, and polymerization proceeds by chain addition of monomer. On the other hand, the AM mechanism proceeds via the addition of molecules containing hydroxyl groups to the activated monomer. This is accompanied by a transfer of charge to regenerate MH^+. During the initial stages of reaction, and in systems with low initial concentration of hydroxyl groups, the ACE mechanism is predominant. However, the presence of hydroxyl groups, i.e., water, polymer chain ends, and comonomer, can favor the AM mechanism. Other reactions include the chain transfer reactions in which an activated chain end reacts with a hydroxyl moiety, water, or alcohol. The transfer reaction via an OH containing compound results in an inactive oligomer, as shown in equation 4:

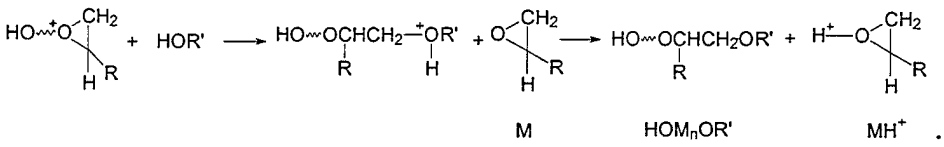

(4)

Initiation of epoxy cationic polymerization using E-beam irradiation is effected using onium salts, like diaryliodonium hexafluroantimonite, that undergo photolysis and release a powerful Bronsted acid. In subsequent steps, this strong protonic acid efficiently initiates the polymerization of epoxy-containing monomer. The mechanism of proton liberation from photoinitiator due to irradiation is summarized in the multistep initiation in equation 5:

$$Ar_2I^+X^- \xrightarrow{h\nu} Ar_2I^+X^{-*}$$

$$Ar_2I^+X^{-*} \longrightarrow ArI^{\cdot+} + Ar + X^- \qquad (5)$$

$$ArI^{\cdot+} + SH \longrightarrow ArI^+H$$

$$ArI^+H \longrightarrow ArI + H^+ \quad .$$

The H^+ ion, produced from E-beam photoinitiation, reacts with the epoxy group of the monomer and produces an active species MH^+ capable of polymerization similar to the thermally cured systems described previously.

We have undertaken an investigation to probe the effect of two alcohols on the polymerization of epoxy resins. The E-beam-induced cationic polymerization of a model epoxy, phenyl glycidyl ether (PGE) in the presence of a primary aliphatic alcohol, 2-cyclohexyl ethyl alcohol (CHEA) and phenol by E-beam irradiation was investigated. PGE was used as a model epoxy because it contains only one epoxy group per molecule; consequently, it polymerizes to linear soluble products that are easily analyzed by size exclusion chromatography (SEC) to provide insight concerning reaction pathways. The effect of CHEA and phenol on network formation was investigated using a low-molecular-weight DGEBA (Epon 825). Epon 825 was used because it forms a crosslinked network upon cationic cure and because it contains little hydroxyl content as a result of its low molecular weight compared to other commercial systems. T_g measurements obtained by DMA were used to assess network structure.

The experiments conducted using PGE and alcohols were designed to gain some understanding concerning the relative rates of reaction of the oxonium ion with an epoxy group vs. that of the oxonium ion with an organic hydroxyl group. The reaction scheme shown in Figure 9 summarizes the complex reaction pathways for a cationically cured mixture of epoxy monomer (M) with an alcohol (ROH).

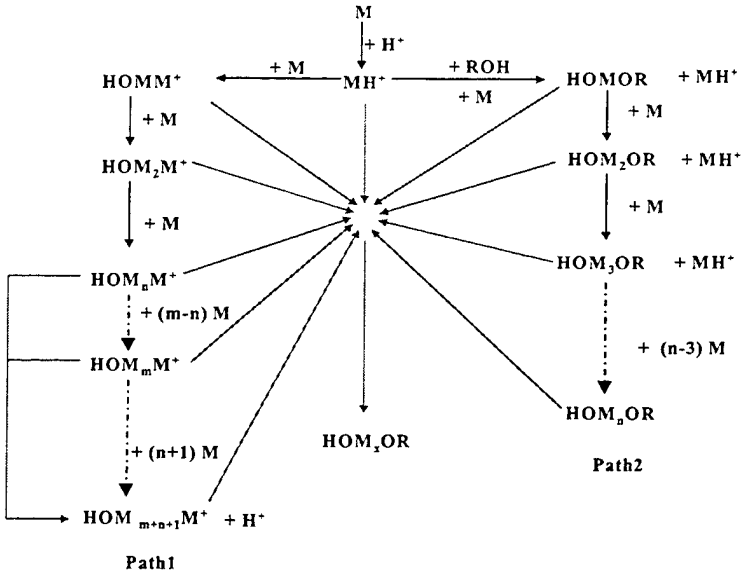

Figure 9. Reaction pathways of cationic polymerization of epoxies in presence of alcohols.

The generation of active center (MH+) is shown at the top of this scheme. The left branch, denoted as path 1, represents polymerization by the ACE mechanism, and the branch to the right, denoted as path 2, represents polymerization via the AM mechanism. The chain transfer reactions are represented by the cross-arrows on the diagram. The molecular weight of products is greatest when the overall reactivity favors path 1. This will happen in the absence of alcohols or when the intrinsic reactivity of the hydroxyl groups of an alcohol with an epoxy active center is much less than that of an epoxy moiety with the same center. In fact, in the case of an equimolar mixture of monoepoxy monomer and alcohol, two limiting cases are apparent. First, if the alcohol-active center reactivity is much less than the epoxy-active center reactivity, then polymer of the highest molecular weight should form. Second, if the alcohol-active center reactivity is much greater than the epoxy-active center reactivity, then only oligomeric products will form and a significant fraction of the alcohol will be consumed.

Polymerization experiments were conducted using equimolar mixtures of PGE and alcohols and reaction products were analyzed using SEC. It was concluded that compared to CHEA the hydroxyl group from phenol is significantly less reactive with the oxonium active center allowing a significant portion of the reaction to follow reaction path 1 in Figure 9. The details of this analysis are given elsewhere [17]. These findings have significant implications regarding the formation of networks in cationically cured multifunctional epoxies. In particular, they show that hydroxyl-containing species, whether derived from

impurities in the system or as part of the monomer system, will significantly influence polymerization and network formation. In addition, the results indicate that the potential exists to tailor the network structure of such systems based on intrinsic differences in hydroxyl group reactivity.

Experiments were conducted using the Epon 825 with varying concentrations of CHEA and phenol to explore the potential effects of varying alcohol reactivity on network formation in diepoxy-based systems. In these experiments, the molar ratio of hydroxyl moieties to epoxy groups was held below 0.2. The difunctionality of Epon 825 leads to the formation of highly crosslinked polymer networks upon irradiation because of the potential for chain propagation at both ends of the monomer. Thus, from the point of view of network structure, the molecule can provide two crosslink nodes. Figure 10 shows the DMA plot of pure Epon 825 after irradiation.

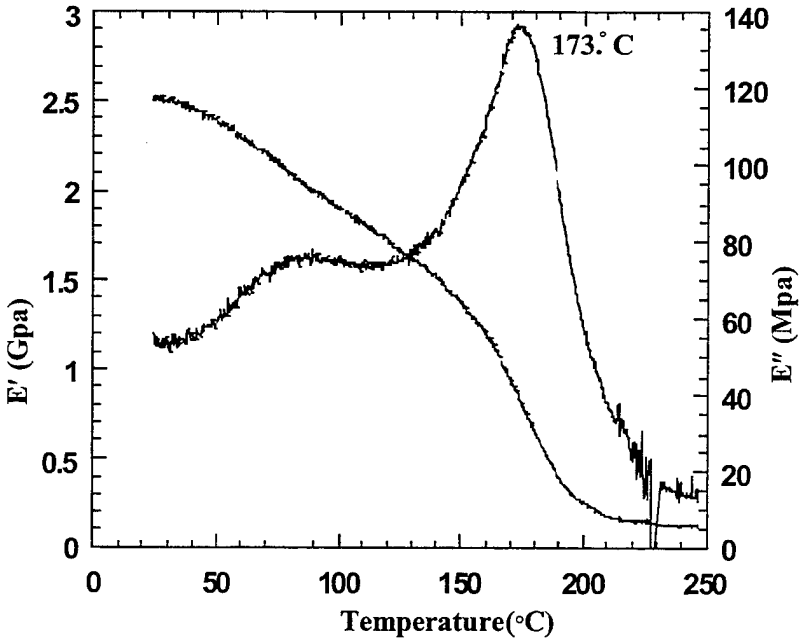

Figure 10. DMA of E-beam-cured Epon 825 showing T_g at 173 °C.

The dependence of T_g on the hydroxyl-epoxy group molar ratio is given in Figure 11 for the CHEA and phenol-modified systems. In both cases, T_g decreases dramatically with increasing hydroxyl content. However, the effect is more pronounced for the CHEA modified system. The T_g depression is consistent with incorporation of alcohols into the polymer network. Every time an alcohol reacts with an activated epoxy monomer, it reduces the crosslinking potential of the system, essentially transforming the diepoxy monomer from one capable of sustaining two crosslink nodes to one capable only of chain extension. Thus, higher levels of alcohol incorporation will lead to fewer crosslinked

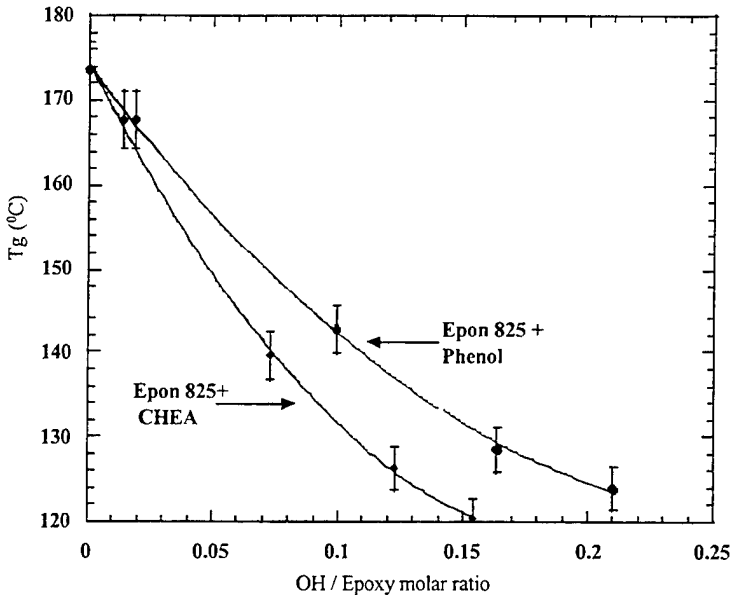

Figure 11. Effect of hydroxyl to epoxy group ratio on T_g of cationically cured Epon 825.

networks and lower T_g. More importantly, the greater reduction of T_g found with CHEA is consistent with the PGE model compound studies which showed that phenol is significantly less reactive than CHEA. In summary, T_g depression associated with incorporating the more reactive CHEA is more pronounced than that associated with adding phenol to Epon 825 at an equivalent hydroxyl to epoxy molar ratio. This suggests that the potential exists to tailor network formation in such systems based on the judicious selection of monomer reactivity and structure. The section that follows describes the development of chain extenders that take advantage of the fundamental understanding of reaction pathways in cationic polymerization.

2.5 Toughened Cationic Resins

The use of chain extenders to toughen thermosetting systems is well known. The challenge in using chain extenders for cationic systems is twofold. First materials that provide adequate chain mobility to enhance yielding while imparting stiffness must be developed, and second, these linear molecules must be incorporated into the crosslinked network. The study previously described provides the basis for designing reactivity of such molecules. Particularly, it was concluded that compounds possessing aliphatic hydroxyl groups (primary or secondary) are highly reactive and are readily incorporated into growing epoxy networks cured by cationic polymerization. Thus linear oligomer/polymers possessing terminal hydroxyl reactivity have been developed as chain extending

toughening agents for cationic systems. These are based on the coreaction of monoepoxies with dialcohols.

Two materials have been synthesized and evaluated. Their backbone structures are based on phenyl glycidyl ether (GP-1) and cyclohexene oxide (GP-2). Both systems have terminal groups possessing aliphatic hydroxyl reactivity. The chain extenders were prepared with a number average molecular weight ~900. GP-1 and GP-2 were added to Epon 825 at concentrations of 10 pph. Previously we showed in Figure 10 the DMA plot for unmodified Epon 825 cured by 20 Mrad. The final T_g of the E-beam-cured Epon 825 system as defined by the sharp loss modulus (E") is 173 °C, although a broad low-T transition is also evident at 82 °C. As with most E-beam-cured systems, the storage modulus (E') below T_g decreases sharply with temperature. The results of material properties for the neat Epon 825 system and the GP-1 and GP-2 materials are given in Table 8. Both GP-1 and GP-2 improve the fracture toughness of the neat resin by 50% while showing no decrease in room temperature modulus and only a slight drop in T_g. The cyclohexene oxide-based chain extender provides a higher T_g than the phenyl glycidyl ether-based system when used at the same concentration. Note that similar formulations based on chain extenders possessing flexible backbones (e.g., polypropylene glycol or polyethylene glycol) would result in materials with severely depressed modulus and T_g. Thus this class of chain extenders provides a promising starting point for developing second-phase-toughened cationically cured epoxy systems.

Table 8. Properties of model epoxy systems toughened using novel chain extenders.

Property	Epon 825	Epon 825 + 10 pph GP-1	Epon 825 + 10 pph GP-2
T_g E" peak (°C)	173	142	152
E' (30°C) (Gpa)	2.5	2.8	2.5
G_{IC} (J/m^2)	67 ± 5	99 ± 5	103 ± 18

2.6 Epoxy-Type Film Adhesives

This task involves evaluation of E-beam-curing adhesive films suitable for composite repair. During this reporting period, eight E-beam cationic adhesive films were developed and tested for single lap-shear strength. In addition, various surface treatments for aluminum substrates were investigated because E-beam has been shown to adversely affect the performance of the bonding layer in treated aluminum.

Aluminum substrates used for testing cationic adhesive require different surface preparation from thermal-curing epoxy adhesives. Most primers used for aluminum surface preparation of thermally cured systems are epoxies containing amine-curing agents. Since E-beam-curing cationic systems are not compatible with amine-curing agents, conventional primers, such as BR127, cannot be used

to prime aluminum surfaces for E-beam bond characterization. Other primers, such as METLBOND 6726, are epoxy wash and do not contain amines, rendering them highly compatible with E-beam processing. However, some of these epoxy-wash systems degrade under E-beam irradiation and frequently exhibit lower protection limits against harsh environments. For the current cationic adhesive screening, we elected to bond onto bare aluminum or silane-treated aluminum surfaces. A combination of two surface treatments, Forest Product Lab (FPL) and phosphoric acid anodized (PAA), was applied on the aluminum prior to bonding. FPL is a sulfuric acid sodium dichromate etch and is stable without primer. PAA is applied on top of FPL-treated aluminum surfaces. PAA is reported to produce a stable oxide surface for up to 72 hr prior to bonding. Fortunately, the screening for cationic adhesives does not involve corrosive conditions, but rather room-temperature characterization. The second treatment explored is the Strategic Environmental Research and Development Program (SERDP)-sponsored Sol-gel treatment. Sol-gel is a more expensive surface treatment and is stable for only 24 hr prior to bonding. However, previous explorations in the Composites Affordability Initiative (CAI)* have qualified this approach to characterizing E-beam-processed adhesives. Therefore, our data will be easy to compare with results obtained by the CAI.

All of the cationic-cured E-beam film adhesives were developed by Applied Poleramic Inc.,† a subcontractor to Northrop Grumman Corporation. Each adhesive film was approximately 10 mil thick without scrim support. The formulation specifications are shown in Table 9. These cationic films are composed primarily of cycloaliphatic epoxide—a highly reactive monomer—and the chain-extending diol bisphenol-A. Formulation EBA-8 is similar to EBA-3 with a slightly larger concentration of anhydride. These formulations explore the impact of anhydride in the cure process under E-beam irradiation, a phenomenon that has not been characterized experimentally. EBA-6 and EBA-7 contain GP-2 and GP-1, respectively. Recall that GP-1 and GP-2 are both di-hydroxy terminated oligomers designed to increase the flexibility of the E-beam-processed matrix by decreasing the crosslink density in the network. The remaining compounds in these adhesive films are viscosity modifiers and tackifiers that allow the formation of room-temperature stable films. Additional small quantities of activation materials, such as phenol, are included to increase reactivity during the early stages of E-beam processing, although these activators reduce the room-temperature shelf life of the films.

---

* CAI is a large Air Force program exploring new composite technologies, including E-beam.

† 850 Teal Ct., Benicia, CA 94510-1249.

Table 9. E-beam-curing adhesive formulations.

Additive	EBA-1	EBA-2	EBA-3	EBA-4	EBA-5	EBA-6	EBA-7	EBA-8
C Aliph Epoxy	25	20	30	10	–	10	10	30
Solid Bis-A	61	72	65	65	60	65	50	60
B-OH	–	5	5	–	–	–	–	5
Phen	–	2.8	1.5	–	–	–	–	1.5
Mthpa	–	–	3	–	–	–	–	5
605	–	–	–	15	30	–	–	–
TEP	12.5	–	–	10	10	10	10	–
DPI	1.4	2.8	2.8	2	2	2	2	2.8
GP-1	–	–	–	–	–	–	30	–
GP-2	–	–	–	–	–	15	–	–
6040/430	1/0.5	0.3/0.1	1/0.5	1/0.5	1/0.5	1/0.5	1/0.5	1/0.5

Because these film adhesives are in development, very little effort was invested in obtaining adhesives that "wet" the aluminum at low temperatures. Rather, these films were subjected to light heating and pressure (180 °F for 30 min) in a press during lap-shear assembly. The pressure was applied to reduce the film thickness to 50% of the initial thickness. Heating these films increased both the flow viscosity and the wetting capability of the films and allowed uniform bondline control to be achieved in all of the sample materials. The final bondline thickness is 5 mil. After cooling, the lap-shear panels that are E-beam processed (namely EBA-1, EBA-2, and EBA-3) were taped tightly to minimize contact stresses resulting from handling, and the lap-shear samples were shipped to Steris Corporation* for E-beam curing. The green strength of the assembled film adhesive joints is less than 500 psi prior to E-beam cure.

Because these adhesives are consolidated in the laminates, no additional pressure is applied during the E-beam-curing step. Consequently, if the films are rapidly processed and the aluminum panels heat prior to C-stage or gelation of the film adhesives, then debonding of the aluminum plates would be expected. Therefore, we elected a slow-dose curing profile that minimizes the heating in the bondline. The cure dose applied is shown in Figure 12. The delay between passes was included to prevent overheating of the specimens and to allow processing to occur using the normal throughput manner of the E-beam source. The large surface area produced adequate ambient temperature cooling between passes during the staging of the adhesives in steps 1 and 2. Based upon earlier experiences, the adhesives will have achieved sufficient cure after two passes to cause gelation, which will result in strong bonds during the remaining cure steps. The cure rate is increased for steps 3–5 to ensure complete conversion and moderate heating in the adhesives. The total energy dose was 150 kGy.

* 2500 Commerce Dr., Libertyville, IL 60048-2494.

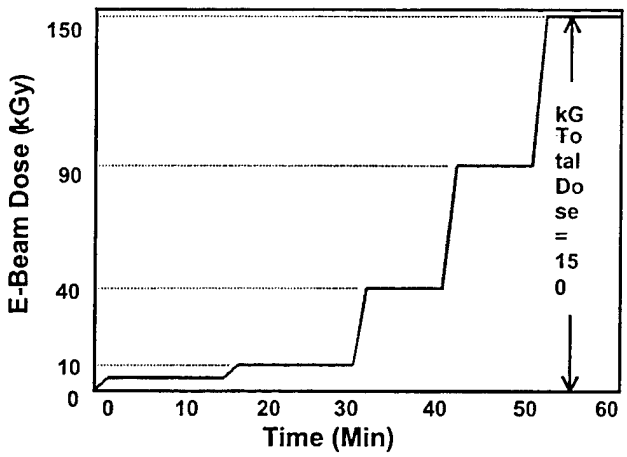

Figure 12. Slow-dose E-beam cure profile for cationic-epoxy film adhesives.

The remaining adhesive formulations (EBA-4, EBA-5, EBA-6, EBA-7, and EBA-8) were received too late for inclusion in the E-beam run. We therefore evaluated these materials by thermal screening. These adhesives were thermally cured at 250 °F and 40 psi for 2 hr. If the lap-shear strength of the thermal system is promising, it will be selected for further curing using E-beam. In addition to the E-beam-curing adhesives, control lap-shear specimens using FM73 were fabricated to validate the aluminum surface treatments. FM73 film adhesive baselines were cured in a press at 250 °F and 40 psi for 2 hr, according to manufacture recommendations.

Results of the room-temperature lap-shear strength of the E-beam-curing adhesive and FM73 control are shown in Table 10. The lap-shear strength of FM73 treated with FPL/PAA is acceptable, and the failure mode is 100% cohesive. This result suggests that the surface treatment is adequate for the aluminum adhesive testing. EBA-3 showed much lower lap-shear strength for the Sol-gel treated aluminum surface preparation. Thermally cured EBA-3 is slightly higher (7%) than the thermal/E-beam-cured specimens. The 2% increase in the anhydride concentration of EBA-8 leads to a dramatic 22% increase in lap-shear strength. Figure 13 is a bar chart of lap-shear strengths for the tested adhesive films. Both EBA-4 and EBA-8 lap-shear values are about 96% of those of FM73. The failure modes for most of the E-beam-curing adhesives are adhesive, not the desirable cohesive failure. The only cohesive failure mode observed for the E-beam-curing adhesive film is EBA-7, which contains GP-1 oligomer. The room-temperature lap-shear values are low for EBA-6 and EBA-7, which is considered to be due partly to the brittle nature of the film. According to Applied Poleramic, the film viscosity for EBA-6 and EBA-7 was not optimized. During the lap-shear panel preparation, small pieces of the films broke off, hindering the fabrication of EBA-6 and EBA-7. In the future, Applied Poleramic will optimize the handling characteristic of the two adhesive systems, to decrease sample preparation variability.

Table 10. E-beam-curing adhesive properties.

		EBA-1	EBA-2	EBA-3	EBA-3	EBA-3	EBA-4	EBA-4	EBA-5	EBA-6	EBA-7	EBA-8
Surface Treatment		FPL/ PAA	FPL/ PAA	FPL/ PAA	FPL/ PAA	Sol-Gel	FPL/ PAA	FPL/ PAA	FPL/ PAA	FPL/ PAA	FPL/ PAA	FPL/ PAA
Cure		Ther/EB			Thermal			Ther/EB	Thermal			
Individual Measurements	A	–	–	–	–	–	4420	–	3259	–	–	–
	B	–	2508	–	3234	1910	4434	–	3501	1036	2145	4211
	C	1546	2372	3094	3184	1992	4262	4054	3461	1097	2513	4494
	D	1808	2223	3308	3680	2834	4081	4338	3386	1356	2640	4211
	E	1976	2597	3344	3751	2380	4737	3964	3449	1725	2498	4215
	F	2138	2883	3516	3964	2788	4401	3815	3449	1842	2607	4632
Average		**1867**	**2516.6**	**3316**	**3563**	**2381**	**4389**	**4043**	**3418**	**1411**	**2481**	**4353**
Std. Dev.		253	249	173	340	431	217	220	86	363	197	198
Failure Mode		A[a]	A	A	A	A	A	A	A	A	C[b]	A

[a] A = Adhesive.

[b] C = Cohesive.

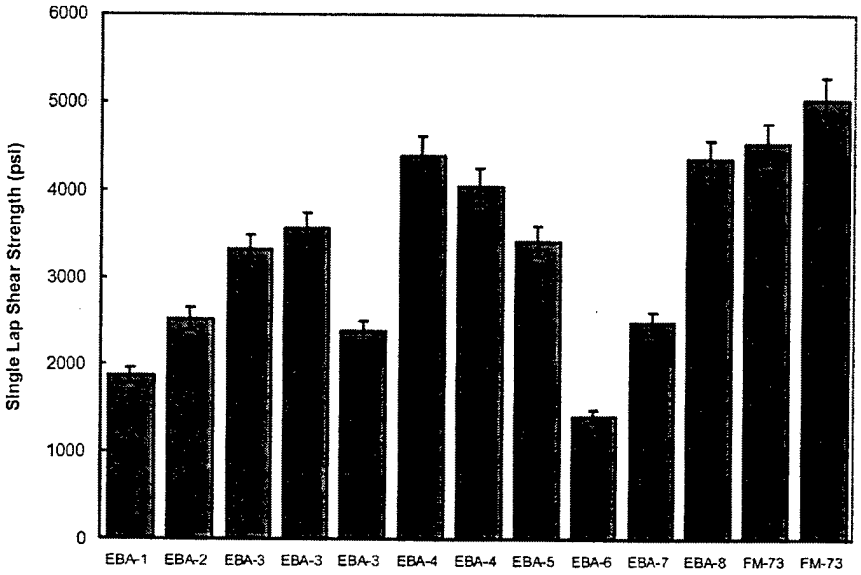

Figure 13. Lap shear strengths of film adhesives on FPL/PAA treated aluminum.

2.7 Simultaneous IPN Film Adhesives

In addition to evaluating true homopolymer-cationic-cured epoxy E-beam adhesives, we also explored E-beam processing of hybrid designs based on simultaneous cure of the IPN structural adhesives. This novel approach uses the DPI initiator to cure the epoxy matrix while E-beam simultaneously excites free-radical propagation in the methacrylate matrix. This approach was previously depicted in Figure 1 and results in one-step-processed IPNs. The monomer

blend consists of two independent networks that cure simultaneously by E-beam processing.

To improve performance, we screened adhesive composition by curing a series of FR/Cat-Epoxy blends with E-beam. We attempted to screen these hybrid materials using thermal curing but recognized early in our efforts that the cure rate variation between the two network types produced inconsistent extent of cure in the two networks. We believe that the differences between network cure conversion could be optimized for thermal cure by selection of the free-radical initiator. However, both concentration and initiation temperature are variables, making this determination a non-trivial effort. Therefore, we cured the materials directly with E-beam and evaluated the extent of network conversion based upon diamond-tip ATR-FTIR and DMA. The results from this study are still undergoing evaluation; however, it is significant to note that one composition of these hybrid IPN structures resulted in a high-T_g and micromechanically linked network, while all other compositions produced independent networks with cure-dependent T_g performance. The unusual characteristic of single-network relaxation occurred for a 50/50 weight blend of monomers, which is 40/60 mole fraction (FR/Epoxy) of difunctional monomers.

We previously attempted an adhesive film experiment (JCAT1) that demonstrated excellent lap-shear performance [6]. By coincidence, the formulation of JCAT1 is very close to the optimized concentrations determined in the recent screening. JCAT1 adhesive demonstrated lap-shear strengths of 3800 psi and a T_g of about 150 °C, even though the adhesive is not toughened using traditional methods, but is comprised solely of an IPN architecture. Figure 14 is an example of second-heat DMA characterization of simultaneous interpenetrating polymer network (SIN) adhesive formulations. All of these systems except M60/40eb demonstrate a high-T_g component at about 150 °C, as well as a low-T_g component between 50 °C and 100 °C. The previous analyses on SeqIPNs pointed to the epoxide fraction contributing to the high T_g matrix, while the free-radical-cured acrylic produced the lower T_g fraction. However, this analysis resulted from second-stage cure of the acrylic in the presence of a fully reacted epoxy-amine system. We have not be able to discern which network is responsible for the high-T_g performance in the SIN formulations, but based upon the compositional study, the formalism of assigning the high T_g to the epoxide matrix would seem reasonable in these materials as well.

Among the unique features of the SIN formulations evaluated by DMA is the occurance of a single T_g transition at approximately 150 °C for the sample composed of 40/60 mole fractions of methacrylate and cationic epoxide. This is a rather surprising result, as all of the other formulations produce two T_g transitions—one for each of the networks in the SIN. Upon characterization of the M40/60eb sample, a further investigation was performed by using frequency sweep characterization. Again, only a single transition is observed for the

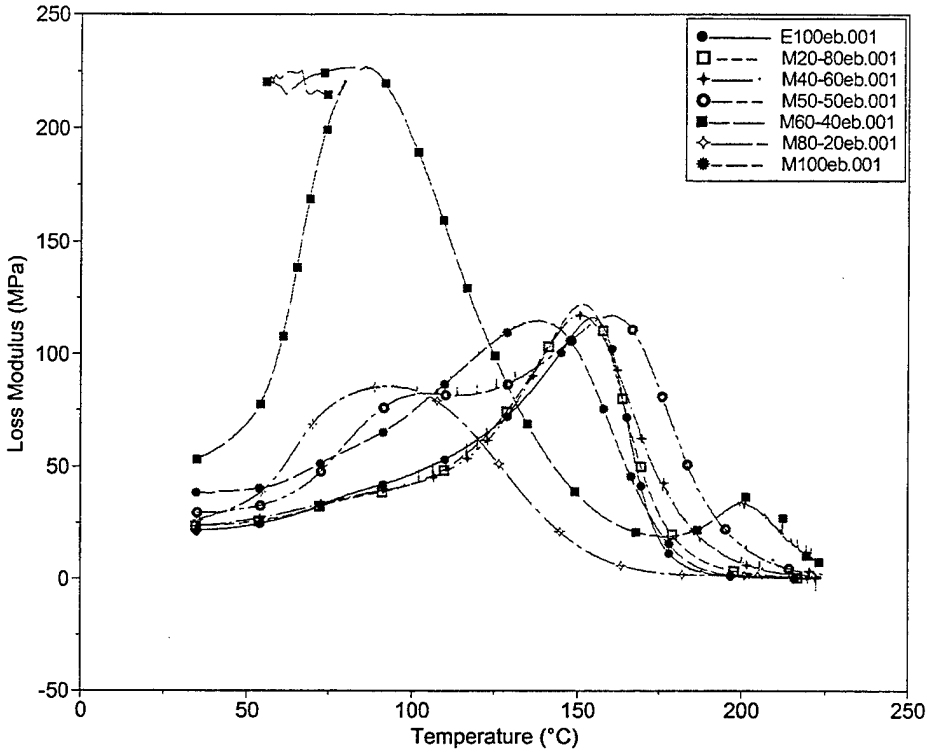

Figure 14. DMA evaluation of SIN formulations on second heat at 1 Hz.

sample, which is similar to results obtained for thermal cured and E-beam cured epoxides of Epon 828. We have not determined the reason for this unique behavior at this time, but investigations are ongoing into the SIN matrix formation during E-beam cure.

2.8 Cationically Cured VARTM Composites

Two basic technologies for VARTM resin formulation have been used to achieve ambient gelation with E-beam cure/post-cure. One type is Lewis acid ambient cure with a cationic E-beam post-cure. The other is an amine/epoxy cure with an E-beam free-radical post-cure. In Northrop Grumman's VARTM evaluation efforts have concentrated on the Lewis acid/cationic curing technology. Both one- and two-part cationic VARTM resin systems were formulated. The advantage of a two-part system is that the shelf life of the resins is infinite. The resins are mixed at a certain ratio at room temperature prior to injecting into the tool. Once the two parts are mixed, the working time of the resin is comparably shorter than that of a one-part system. One early two-part cationic VARTM formulation, VEB-11, exhibited a long working life at slightly elevated temperatures and multi-day (>2 days) shelf life at room temperature after blending. The viscosity of VEB-11 increases dramatically after 90 min at 40 °C,

reaching 1300 cP in 2 hr, which is a viscosity outside of VARTM process windows. However, up to 90 min, the viscosity is very low and allows filling of fabric molds by VARTM.

Additionally, a one-part system, VEB-7, was prepared to meet additional requirements for field repair conditions. The viscosity of VEB-7 at room temperature was 1000 cP, which was too high to allow for room-temperature injection. The resin was heated to 40 °C prior to degassing and injected into a heated AS4 fabric preform at 50 °C, which reduced the flow viscosity to below 500 cP. Once the injection was completed, the assembly was cured using an E-beam dose rate of 5 kGy/pass to a final cure dose of 150 kGy. The short beam shear (SBS) and 3-point flexural data under different testing conditions are listed in Table 11. The 180 °F/wet flexural strength shows less than 60% property retention, which might be due to the slow curing dose rate, although this loss in performance is consistent with other cationic-cured E-beam resins.

Table 11. Mechanical properties of 150 kGy E-beam-cured AS4/VEB-7 composites.

	Flexural Strength (ksi)	Flexural Modulus (Msi)	SBS Strength (ksi)
Room Temperature/ Ambient (RTA)	108	9.3	6.0
180 °F/wet	63	9.1	4.7

Figures 15 and 16 show the flexural properties and SBS strength comparisons of VEB-7 and VEB-11. VEB-11 is catalyzed by a Lewis acid, which is added to allow gelation to take place at room temperature. Part B of VEB-11 also contains an acrylic, which is a liquid carrier for the catalyst. The two-part curing VEB-11 system flows better at room temperature and produces cured resin with less stiffness compared to the one-part system. For the one-part system, the curing agent is DPI, which produces resin with higher stiffness. This is evidenced in the flexural modulus of VEB-7, which is 5% higher than that of VEB-11.

2.9 Cationic Epoxide Cure for Prepreg Formulations

Reformulation of the E-beam-curing cationic resin and associated adhesive to extend the toughness, durability, and thermal performance to meet 250 °F/wet service for aircraft repair and remanufacturing continues to be a limiting aspect of cationic cured E-beam resins. Although the T_g of the prepregging resins meets the required goal of 250 °F/wet service, the cationic resins still lack interlaminar strength and toughness. The basic problem is in the cure mechanism of E-beam

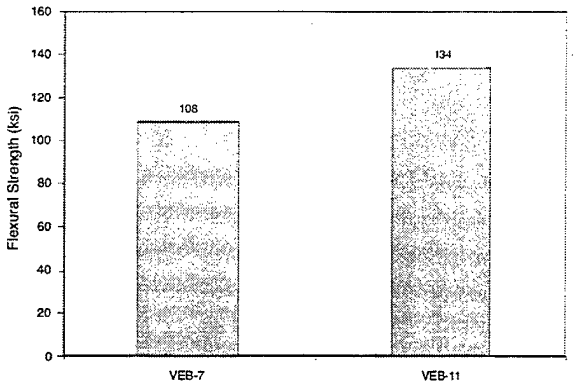

(a) Strength

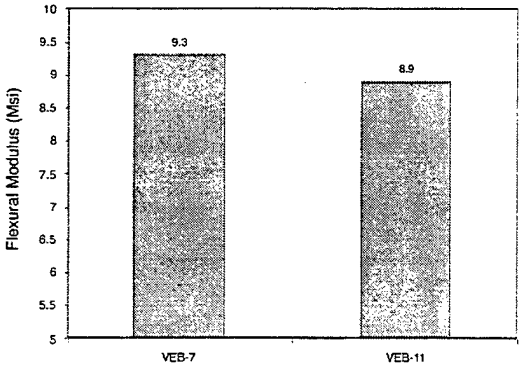

(b) Modulus

Figure 15. Comparisons of E-beam-cured resins VEB-7 and VEB-11.

resins. Unlike thermal resins, for E-beam resins, there is only one choice of catalyst type with a resulting homopolymerization mechanism. Until the discovery of the impact of alcohols on network structure reported earlier in this document, there was no epoxy coreactant available to introduce flexibility in cationic-cured matrices. The high crosslink densities of E-beam-cured systems produced both brittle networks and high glass transition temperatures in composites. However, performance is still a handicap to implementing these materials in aerospace applications.

2.10 Thermal Screening and Baseline Performance for E-Beam Prepregs

A new prepreg system, AS4/CAT-M unidirectional prepreg, is used to investigate baseline performance of cationic epoxide systems cured on moderate modulus carbon fibers. The prepreg provided by YLA, Inc.* has a net resin content of 36.8% by weight. Investigation of processing and cure specific details

* Bay Vista Ct., Benicia, CA 94510-1123.

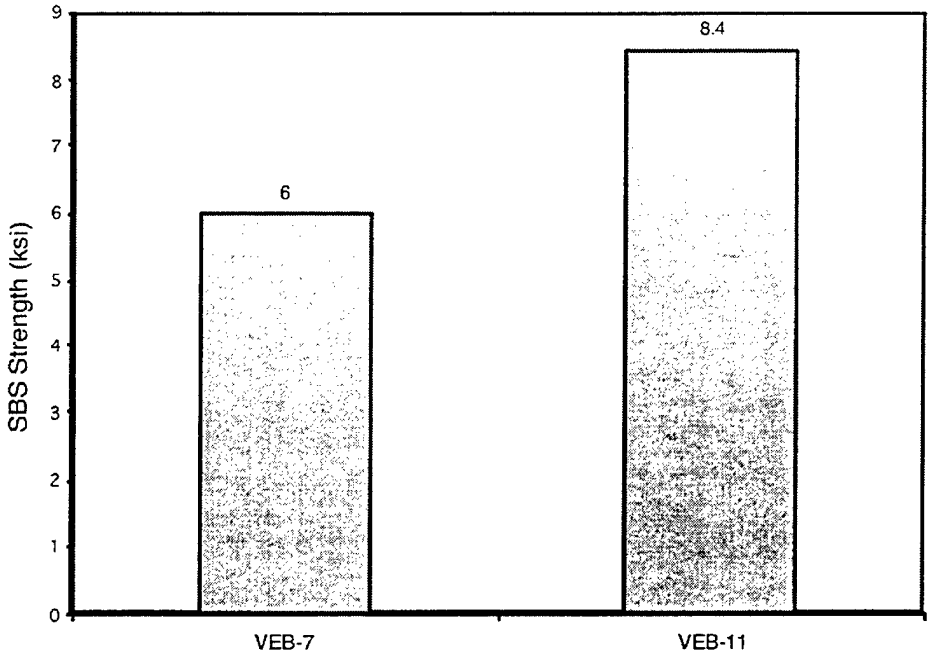

Figure 16. SBS strength of E-beam-cured resins.

are determined by DSC analysis. A thermal cure is used to baseline the materials performance under various processing conditions, including vacuum and autoclave consolidation.

DSC analysis was carried out at a heating rate of 10 °C/min from ambient temperature to 300 °C. The exotherm peak, as shown in Figure 17, is narrow and sharp, with a peak temperature of 186 °C. These data indicate that the debulking is relatively stable up to temperatures around 130 °C (266 °F).

Three composite panels were fabricated using thermal cure to determine the baseline properties of the AS4/CAT-M composite laminate. Two 7-in × 8-in panels were debulked ply-by-ply at room temperature, producing one 8-ply and one 16-ply panel. The panels were cured under vacuum bag at 160 °F for 1 hr and 350 °F for 2 hr. No external pressure was applied to the panels, beyond vacuum consolidation. For the third panel (16 ply), the cure was completed in the autoclave using a typical epoxy 2-hr cure cycle with an autoclave pressure of 85 psi and a cure temperature of 350 °F.

The three laminates were examined by ultrasound (C-scan) and optical microscopy. Both test methods indicate significant porosity in vacuum-bag-cured laminates. The autoclave-cured laminate exhibited no porosity. Figures 18–20 are photomicrographs of the 16-ply vacuum-bagged laminate, 8-ply vacuum-bagged laminate, and 16-ply autoclave-processed laminate, respectively.

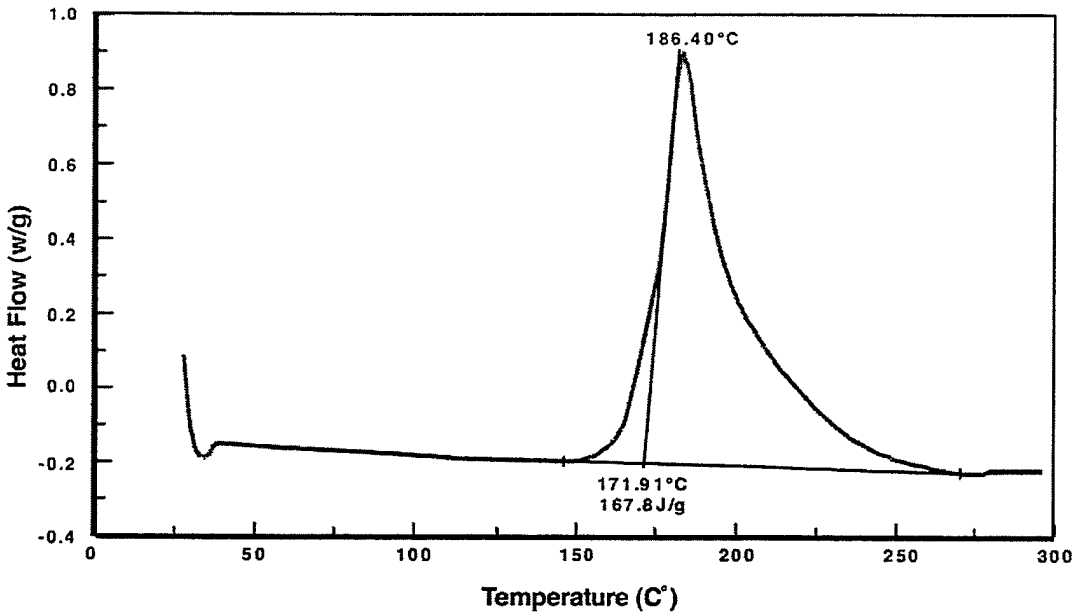

Figure 17. DSC of AS4/CAT-M prepreg.

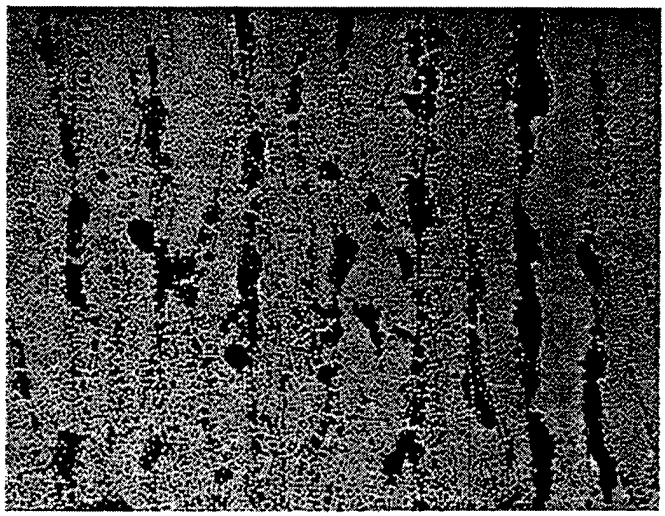

Figure 18. Optical photomicrograph of 16-ply vacuum-bag-cured AS4/CAT-M.

Flexural (0°) and SBS properties of AS4/CAT-M were evaluated under ambient, 180 °F dry and wet, and 250 °F dry and wet conditions. Three-point flexural testing was conducted per ASTM D790 [7], and the SBS strength was determined per ASTM D2344 [18]. Specimens for wet testing were moisture conditioned using a 3-day water boil. The percent average moisture absorption for all specimens is shown in Table 12. Vacuum-bag-cured specimens have 10-20% higher moisture absorption because of the porosity of the laminate, indicating a substantial weakness of E-beam processing methods available at this time.

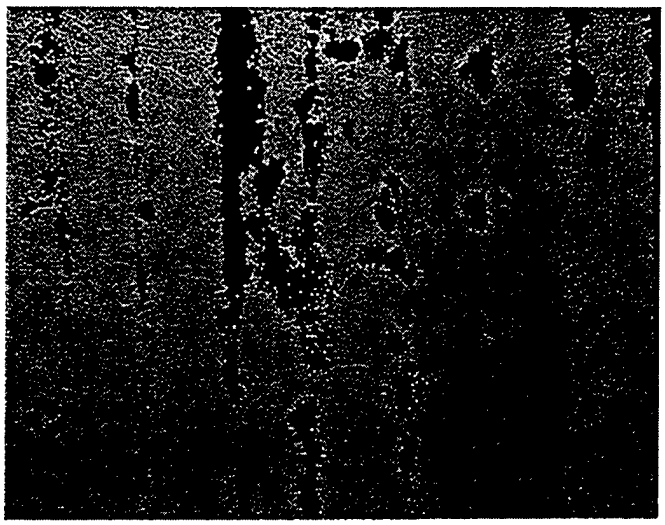

Figure 19. Optical photomicrograph of 8-ply vacuum-bag-cured AS4/CAT-M.

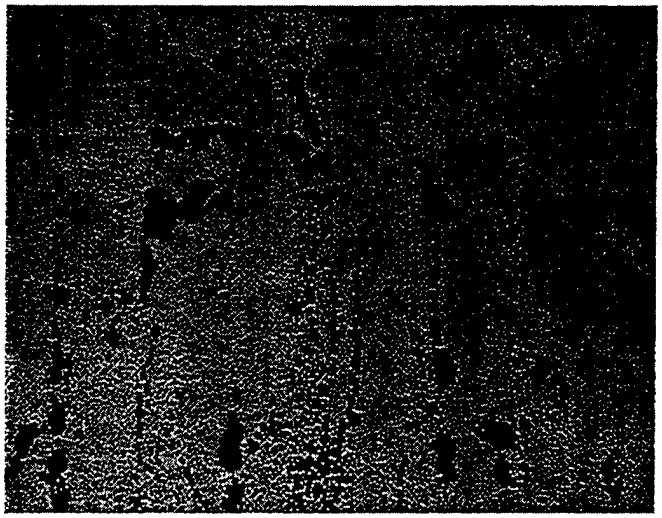

Figure 20. Optical photomicrograph of 16-ply autoclave-cured AS4/CAT-M.

Table 13 shows the SBS strength of AS4/CAT-M under various testing conditions. As expected, vacuum-bag-cured specimens exhibit much lower SBS strength, which is again attributed to laminate porosity. Although the quality of autoclave-cured laminates was excellent, the SBS strength was still lower than an amine-cured epoxy such as 3501-6 (16 ksi at ambient), again owing to poor resin quality, as well as potential interfacial shear problems with E-beam-processed carbon fiber sizing [19].

Table 12. Specimen moisture absorption for AS4/CAT-M laminates after 3-day water boil.

	Vacuum-Bag-Cured Average Moisture Absorption (%)	Autoclave-Cured Average Moisture Absorption (%)
SBS Specimens	0.97	0.80
Flexural Specimens	0.68	0.57

Table 13. SBS strength of as-fabricated and conditioned AS4/CAT-M prepreg laminates.

	RTA Strength (ksi)	180 °F/ Dry Strength (ksi)	180 °F/ Wet Strength (ksi)	250 °F/ Dry Strength (ksi)	250°F/ Wet Strength (ksi)
Vacuum Only	8.2	6.8	7.3	5.1	5.4
	8.6	7.1	7.1	5.5	4.9
	8.2	7.3	7.1	5.4	5.3
Average	8.3	7.1	7.2	5.3	5.2
Std. Dev.	0.2	0.3	0.1	0.2	0.3
85-psi Autoclave Pressure	11.2	9.5	8.5	7.3	6.8
	11.5	9.5	9.0	7.7	6.8
	11.6	9.3	9.0	8.0	7.0
Average	11.4	9.4	8.8	7.7	6.9
Std. Dev.	0.2	0.1	0.3	0.4	0.1

Table 14 shows the flexural properties of AS4/CAT-M. The vacuum-bag-cured specimens exhibit much lower strength and modulus values compared to the autoclave-cured specimens. Additionally, there is a much more drastic knockdown in properties above 180 °F under wet conditions. For instance, at 180 °F/wet, there is 63% strength retention for the autoclave-cured laminate and only 55% for the vacuum-bag-cured laminate. At 250 °F/wet, retention of properties was only 49% and 43% for the autoclave-cured and vacuum-bag-cured laminates, respectively. This suggests that the service temperature of this resin system is only 180 °F/wet maximum, not suitable for 250 °F/wet service.

2.11 E-Beam Processing of Prepregs

After finding low performance in the laminates developed using AS4/CAT-M, a new formulation of toughened resin was investigated. The new prepreg is AS4/T-17, where the carbon fiber is kept constant and an improved toughness resin is prepregged onto the laminate. Laminate processing of AS4/T-17 started with hot debulking at 160 °F for 1–2 hr under vacuum. The best and most efficient way of achieving the final cure is to immediately expose the assembly after the hot debulking stage to E-beam energy to induce complete cure. However, in most cases, the E-beam capability is not readily available; hence, shipping the assembly to an E-beam facility is a common practice. Very often in

Table 14. Flexural properties of as-fabricated and conditioned AS4/CAT-M prepreg laminates.

	RTA Strength (ksi)	RTA Modulus (Msi)	180 °F Dry/Wet Strength (ksi)	180 °F Dry/Wet Modulus (Msi)	250 °F Dry/Wet Strength (ksi)	250 °F Dry/Wet Modulus (Msi)
Vacuum Only	248.7	18.0	196.5/143.4	16.8/16.8	124.1/107.2	17.2/15.7
	243.1	16.9	168.1/137.5	16.5/17.5	−/108.4	−/15.6
	252.8	17.1	−/129.2	−/16.4	−/104.2	−/15.7
Average	248.2	17.3	182.3/136.7	16.7/16.9	−/106.6	−/15.7
St. Dev.	4.9	0.6	20.1/7.1	0.2/0.6	−/2.2	−/0.1
85-psi Autoclave Pressure	253.8	18.0	197.3/166.8	18.2/19.0	171.4/131.7	18.3/17.2
	260.1	17.9	189.6/150.1	18.2/18.0	−/122.8	−/17.4
	256.7	17.7	−/166.8	−/18.0	−/126.5	−/17.4
Average	256.9	17.9	193.5/161.2	18.2/18.3	−/127.0	−/17.3
St. Dev.	3.2	0.2	5.4/9.6	0/0.6	−/4.5	−/0.1

such cases, the hot debulked panels are shipped on the project plate under vacuum to prevent air from infiltrating the layup. In addition to the added shipping cost of this approach, losing vacuum during shipping is common. This results in additional preparation requirements at the E-beam facility where panels are rebagged and hot debulked for an additional hour prior to curing at the E-beam service facility. The vacuum seal is maintained at least through the first high-energy pass under the E-beam curtain, providing a gelled matrix while under consolidation pressure.

To eliminate the requirement for shipping on a project plate and, more importantly, to eliminate the need for additional hot debulking at the E-beam facility, an alternate prepreg material was developed that requires heat to induce flow of the resin. The prepreg layup is fully consolidated after the initial hot debulking process allowing the laminate to be shipped freestanding. The matrix resin contains enough thermoplastic polymer so that the T_g of the prepreg is above ambient. On heating, the resin will flow in the usual manner for prepreg. The increased resin flow also reduces the bulk factor (per-ply thickness of the prepreg) after debulking. The T-17 matrix resin was developed by Applied Poleramic Inc. to add more "memory" to minimize rebound after layup. The viscoelasticity was changed from a previous formulation by increasing the fraction of PES oligomer to 14%. The PES is Radel A-100 predissolved in Epon 332. Table 15 shows the formulation of the T-17 matrix resin. The T-17 resin was prepregged onto AS4 unidirectional carbon fiber tows in 1-ft-wide segments. The per-ply thickness of the prepreg is 6.5 mil. The prepreg quality was excellent and had good tack, despite the higher T_g.

Table 15. Formulation of T-17.

Component	Parts per Hundred
Epon 332	70
Epon 742	22
Zeon 351	3
Coupler (Bis-A epoxy)	2.5
DPI-1 (catalyst)	2.5
Additive	1.5
439 (multifunctional epoxy)	44

Thermal screening is again performed on the prepreg prior to E-beam processing. Upon debulk, a 16-ply layup had an average per-ply thickness of 6.15 mil. The layup was bagged using the double-bag technique. To establish the baseline properties, the 16-ply layup was thermally cured by heating the laminate to 170 °F under vacuum. After the temperature reached 170 °F, the inner bag vacuum was turned off, and the vacuum on the second bag was applied and maintained while heating the laminate to 350 °F. Final cure was at 350 °F for 2 hr. Per-ply thickness of the cured laminate measured 6.06 mil while the photomicrograph in Figure 21 indicates porosity in the center section of the laminate. SBS testing was performed under ambient conditions. The SBS strength was 10.4 ksi, the flexural strength 177.0 ksi, and the modulus 19.6 Msi. The SBS strength is comparable to AS4/CAT-M data; however, there is a reduction of approximately 30% in flexural strength due to the addition of thermoplastic component in the matrix resin.

A second 16-ply laminate was processed using a slightly modified processing cycle to prevent porosity from developing during cure. Using the same double vacuum-bagging technique, the layup was heated to 170 °F and allowed to dwell at that temperature for 1 hr under vacuum. After 1 hr, vacuum on the first bag was turned off, vacuum on the second bag was turned on, and heating was continued to 350 °F for 2 hr. The cured laminate looked excellent, and per-ply thickness was reduced to 5.88 mil, which is comparable to autoclave-cured laminate per-ply thickness observed for AS4/CAT-M. Resin content by weight of 30.9% and fiber volume of 59.1% were determined from acid digestion. There is no substantial porosity in the photomicrograph of the second laminate (Figure 22). The mechanical performance of this panel was also evaluated. SBS strength of 12.19 ksi, flexural strength of 189.46 ksi, and flexural modulus of 17.21 Msi were obtained for the non-porous laminate. A comparison of the SBS and flexural properties of the porous and non-porous laminates is shown in Figure 23. A 7% improvement can be seen for the flexural strength values, but a much greater improvement, 17%, is realized for the SBS strength numbers. This is not surprising; because of the small SBS specimen size, any defects such as porosity in the specimen will result in a drastic decrease in the tested values. Hence the porous laminate suffered a significant loss of performance due to porosity.

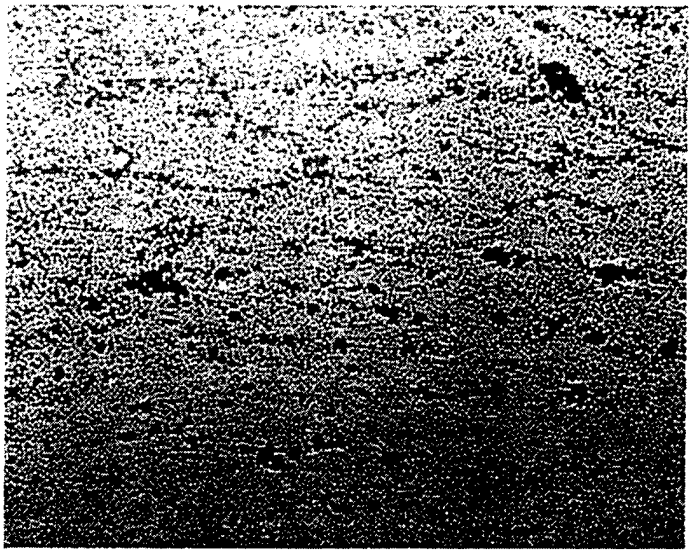

Figure 21. Photomicrograph of AS4/T-17 laminate showing porosity.

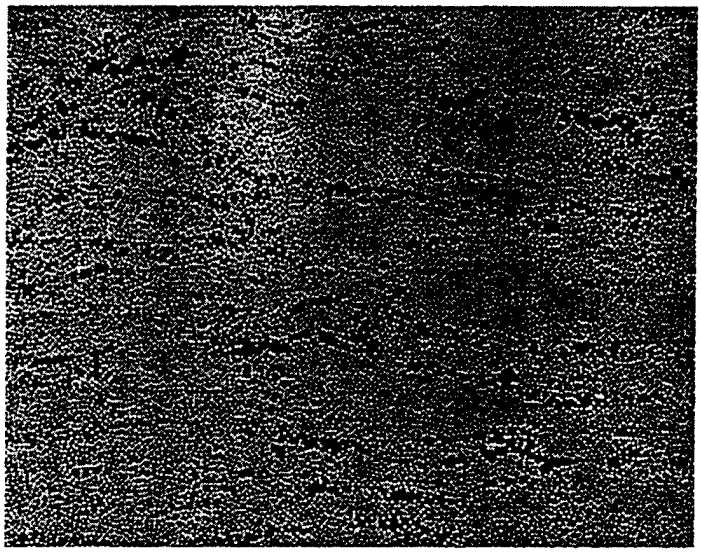

Figure 22. Photomicrograph of AS4/T-17 laminate with improved processing.

Three AS4/T-17 panels were hot debulked in a heated platen under vacuum at 170 °F for 2 hr and E-beam cured at Science Research Laboratory (SRL),* to determine the effect of E-beam-curing rate on the physical and mechanical properties of the laminates. The SRL facility uses a 5-MeV accelerator. The debulk cycle determined previously was employed at the SRL facility to produce three panels. Each panel was removed from the project plate and E-beam cured freestanding on an aluminum back plate. Each panel was cured under different conditions as shown in Table 16.

* 15 Ward St., Somerville, MA 02143.

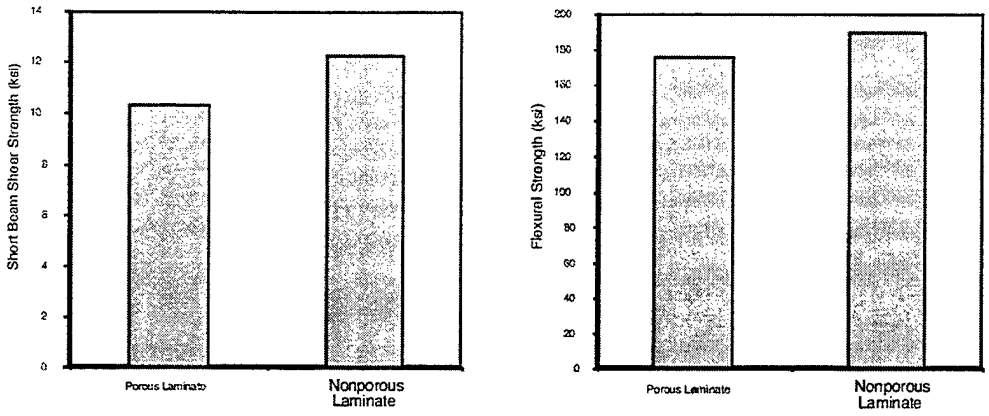

Figure 23. Mechanical property comparison of porous and nonporous AS4/T-17 laminates fabricated using vacuum bag and thermal curing.

Table 16. E-beam-cure parameters for AS4/T-17 composite samples.

Panel Identification	Cure Dose Increment (kGy/pass)	Total Dose Applied (kGy)
A-1	5	150
A-2	5	300
B-1	25	150
B-2	25	300
C-1	75	150
C-2	75	300

To achieve a total E-beam dose of 300 kGy, the panel was first subjected to a dose of 150 kGy, then half of the panel was covered with a thick Al plate to prevent e-beam energy from further curing of the laminate. The E-beam curing was continued to a final dose of 300 kGy. Photomicrographs show that the laminate quality is excellent with no visible voids present.

DMA testing was performed to obtain the glass transition temperature for the E-beam-cured laminates. A peak is evident at around 80 °C in the loss moduls plot, which is known to represent small unreacted molecular units, such as dimers, trimers and n-mers that are not covalently linked to the network backbone. One does not observe any changes in the intensity of the 80 °C peak, even on applying twice the nominal total dose, e.g., at 150 kGy and 300 kGy the peaks are the same. However, the peak is drastically reduced by changing the dose increment from 5 kGy to 25 kGy to 75 kGy per pass. The higher rate of curing resulted in highly crosslinked molecular structures in the composite. Additionally, the increased dose increment does not dramatically impact the final T_g of the resin, which is around 170 °C, but does reduce the low T_g contributions. Figure 24 shows the maximum T_g from high temperature loss modulus transition.

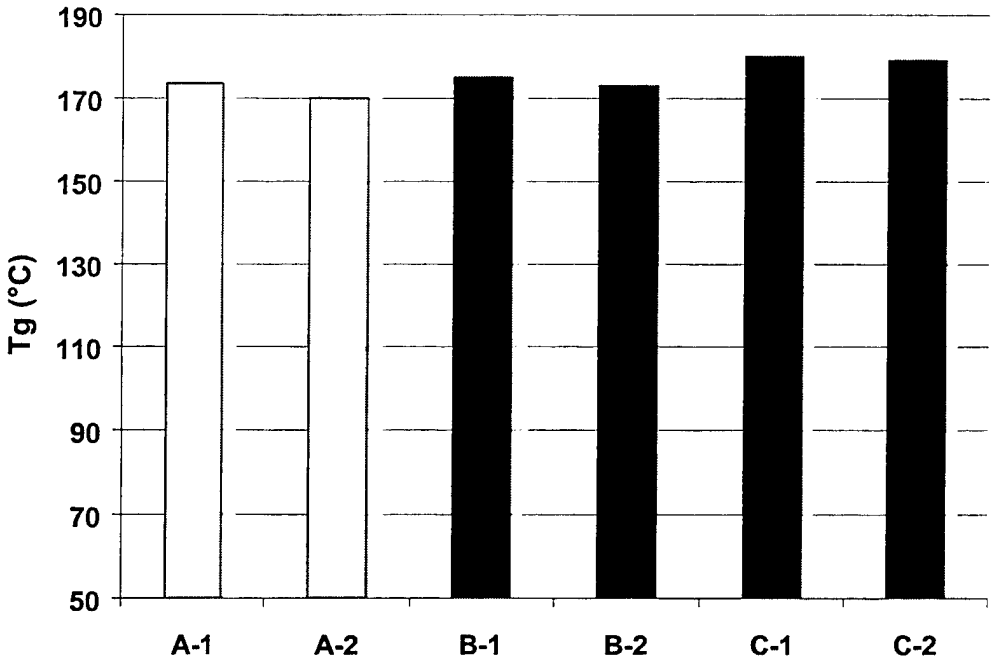

Figure 24. Glass transition temperatures of E-beam-cured AS4/T-17 composite panels cured to 150 and 300 kGy on a 5-MeV accelerator.

DSC data of the composites were also obtained to determine the effect of E-beam dose increments and total dose on extent of cure for the AS4/T-17 composite. Composites A-1 and B-1 exhibit a small residual exotherm at 100 °C and 120 °C, respectively, during the first scan. Laminate C-1 also exhibits a small exotherm on first heat. Upon second ramp, the specimens show no additional exothermic events. Additionally, the reduction of the exotherm peak from the DSC data correlates well with the reduction of the α peak from DMA data for panels cured with a low dose rate to high dose rate. Therefore, the exothermic event may be attributed to further reaction of activated polymer chain ends on heating.

To determine the mechanical integrity of the E-beam-processed laminates, 30 specimens from each panel were machined to 1 × 0.25 in for SBS testing. Prior to testing, two-thirds of the specimens were conditioned using a 3-day water boil for hot/wet testing. Moisture uptake as a fraction of sample weight for the conditioned specimens is listed in Table 17. Figure 25 shows a bar chart of the moisture pickup for each set of specimens.

Percent moisture absorption for specimens from panel C is much lower than for specimens from panels A and B, with panel C coupons absorbing 50% less water. It appears that the high irradiation dose increment produces more highly cross-linked networks in panel C. The higher does rate results in a significant temperature rise in the panel during cure, resulting from the exothermic cure

Table 17. Absorption of moisture-conditioned specimens.

	Day 1 (% Gain)	Day 2 (% Gain)	Day 3 (% Gain)
A-1	0.46	0.51	0.59
A-2	0.52	0.54	0.65
B-1	0.35	0.45	0.55
B-2	0.40	0.54	0.63
C-1	0.27	0.33	0.35
C-2	0.20	0.25	0.33

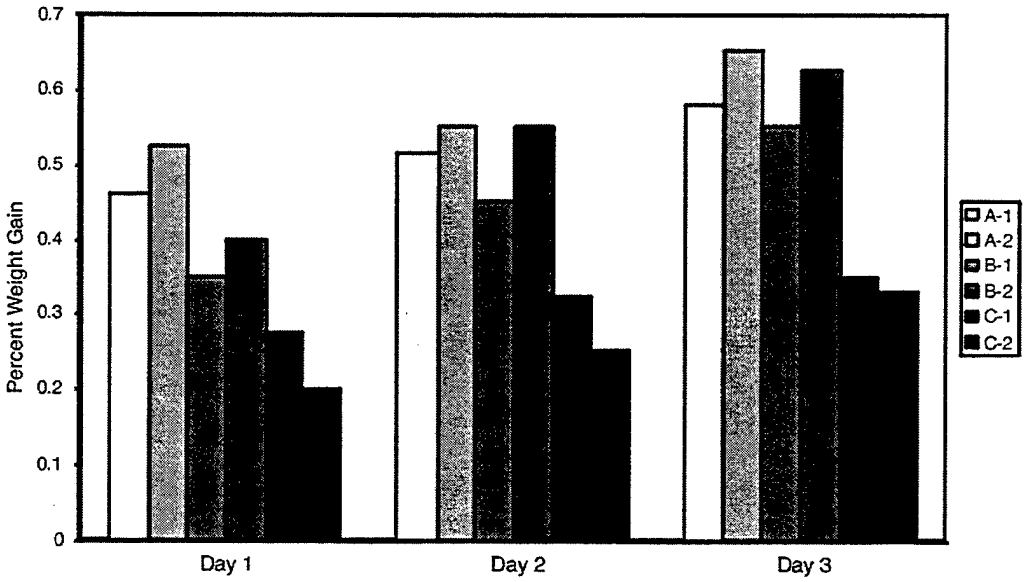

Figure 25. Moisture absorption of SBS specimens.

process and the E-beam heating energy. This result suggests that a higher dose increment can produce more complete reactions, which is partially substantiated by the small and zero exotherm energy of panel C resins in the DSC characterization. The combination of the high dose rate and the chemical exotherm produces a molecular network that is much more efficient, and a panel with a smaller free volume. Since the moisture uptake of a composite laminate is closely related to the free volume of the panel, a smaller weight gain for laminates C-1 and C-2 is reasonably expected. SBS testing was conducted using ASTM D2344 [18] at room-temperature/dry, 180 °F/wet, and 220 °F/wet conditions. The data are shown in Figure 26. A minimum of five specimens was tested for each condition.

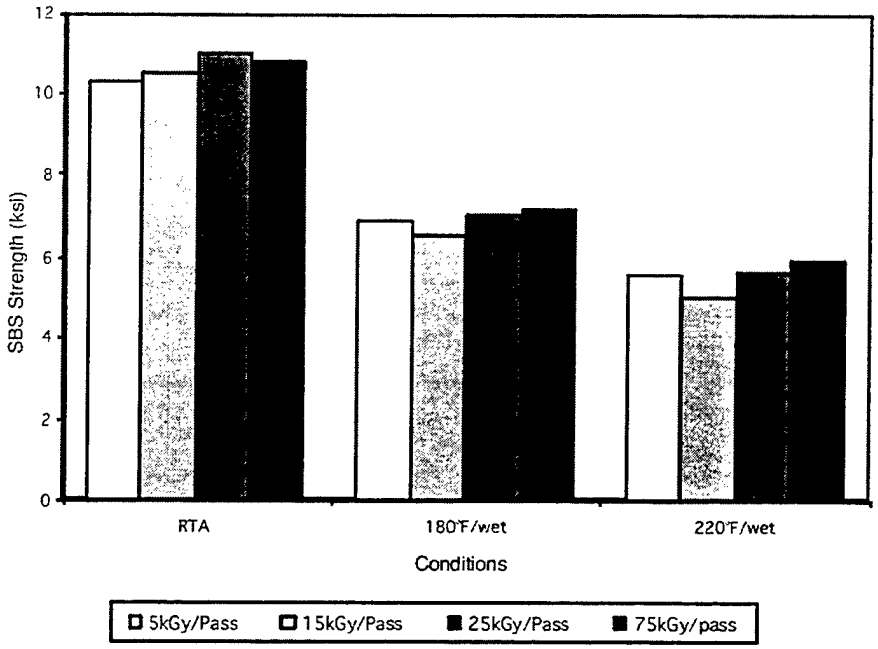

Figure 26. SBS strength of E-beam-cured AS4/T-17 composite laminates.

In addition to the three aforementioned laminates, an AS4/T17 laminate was E-beam cured at Acsion Industries* using their 10 MeV machine at a curing dose of 25 kGy/pass for a total dose of 150 kGy. The SBS data for this laminate were also shown in the figure. In almost every condition, SBS strength increases with dose rate. Although the increase is not huge (about 7.5% from 5 kGy to 75 kGy for 220 °F/w), the trend is consistent.

For the AS4/T-17 laminate cured at 25 kGy/pass, flexural properties were also determined at RTA, 180 °F/wet, and 220 °F/wet as shown in Table 18. The wet specimens were conditioned in 3-day water boil. The 3-point flexural testing was conducted according to ASTM D790 [7]. The average data were based on three specimens, and the modulus was taken between 10 and 40% of the ultimate load. Hot/wet specimens exhibited good retention of properties compared to the room-temperature specimens.

Table 18. Flexural properties of AS4/T-17 cured at 25 kGy/pass.

	RTA	180 °F/wet	220 °F/wet
Strength (ksi)	183	167	157
Modulus (Msi)	18.4	17.8	18.1

* P.O. Box 429, Pinawa, Manitoba, Canada ROE ILO.

Three additional resin formulations (M30, M32, and M33) were prepared for improving resin toughness. M30 is a cationic epoxy with polyethersulfone (PES) oligomer. M32 and M33 are multifunctional cationic epoxies with Perstorp's dendrimer. The three curable resin systems were prepregged with AS4 fibers and subjected to two different total dose E-beam cure cycles, 80 kGy and 150 kGy. The cured unidirectional laminates were then tested for SBS strength (Table 19). The SBS strength of these resin systems did not show improvement over the work with earlier E-beam curing epoxies. SBS values were still around 10 ksi and far from the 13–15 ksi typical of thermally cured epoxies.

Table 19. SBS strength of cationic resins.

	M30 (80 kGy)	M30 (150 kGy)	M32 (80 kGy)	M32 (150 kGy)	M33 (80 kGy)	M33 (150 kGy)
Strength (ksi)	8.6	9.4	9.5	10.3	9.3	9.3
St. Dev.	0.4	0.3	0.2	0.1	0.2	0.4

2.12 Vacuum Bag Consolidation of Adhesive Materials

We have already demonstrated in the previous screening discussion that vacuum consolidation produces insufficient quality of laminates for some high-viscosity prepreg systems. This result is further investgated for adhesive materials. The importance of the processing on adhesive performance begins to increase as the potential for field-level applications of these systems is approached. Most of our developments for screening of E-beam adhesives have progressed using a hot-press and light positive pressure (5–15 psi) to obtain consolidation and achieve uniform bondline thickness. Recently, however, we learned of unusual processing conditions being applied under the CAI. The CAI group implemented a cure schedule that included layup of the adhesive panels followed by vacuum-bag consolidation and oven staging. We had not previously considered the impact of negative pressure on adhesive performance and therefore were surprised by the results presented on ADEP01 evaluated under the CAI. Consequently, we undertook a simple analysis of the performance of adhesives cured under both positive and negative consolidation pressure.

Initial screening of vacuum-bag consolidation involved characterization of performance knock-down of a commercial paste adhesive (Hysol EA9394) when processed under vacuum. We prepared a group of lap-shear panels under both light positive pressure (15 psi) and full vacuum pressure (14 psi or 30-mm Hg). The results of this test demonstrated at least a 20% knockdown in the performance of the commercial system when processed using vacuum consolidation.

Following the commercial paste demonstration, we evaluated green strengths in ADEP01 cured under the same two consolidation conditions. Previously, we

showed that ADEP01 possessed a good green strength at 1000–1200 psi using positive pressure. Upon curing in vacuum, we observed a substantial loss in performance to 400–600 psi. These reductions in performance are consistent with CAI results, where final strengths of ADEP01 achieved only 1200–1600 psi. We also experienced knockdown in performance on a series of modified ADEP01 adhesives that achieved low lap-shear strengths with E-beam cure.

Fortunately, the loss in performance resulting from vacuum processing is a common difficulty with adhesives. We therefore determined the primary sources for these performance losses in ADEP01 and prepared materials to compensate for the vacuum impact. The most common method of improving performance is to decrease the volatile concentration in the adhesives. Unfortunately for our situation, ADEP01 is formulated to be a non-volatile organic compound (VOC)-emitting resin and therefore does not possess highly volatile monomers. The second approach is to change the viscosity of the adhesive components. This second approach is achieved by forming an adduct phase of the amine-component with much higher molecular weight epoxides. The adducts possess partially reacted amines that are much less likely to bloom to the interface of the aluminum when negative pressure is applied. We optimized the adduct formation by formulating to an amine-rich resin with good spreading viscosity.

Last, we recognized that most of the trouble with vacuum consolidation results from expanding air bubbles in the adhesive pastes. These air bubbles are incorporated into the resin phase during the blending of part A and part B in the two-part systems. Since the IPNs are developed using two-part epoxy-amine chemistry, we are unable to eliminate this mixing step. However, the art of adhesive application has been greatly advanced in the last 10 years by the introduction of meter-mixing tools, such as the MixPac. These mixing units enable measuring and mixing of adhesive pastes in a high-shear low-air environment. The adhesive components are injected from a two-channel syringe into a mixing tube. With continued application of pressure on the syringe, the resin components are pressed down the mixing tube and are shear blended until the two components exit the nozzle end of the mixing chamber as a single blended resin. These tubes provide unique ability to blend moderate viscosity two-part paste adhesives with very little incorporation of air on blending. The elimination of air from the adhesives results in greater retention of performance during vacuum-bag processing.

From these negative pressure consolidation studies, we have determined a number of methods for reducing air entrapment in our adhesive pastes. We therefore can proceed with our development of paste adhesives for E-beam cure with confidence that vacuum processing of these materials will be an option once formulations are optimized.

3. Application of E-Beam Technology in Military Systems

3.1 Composite Integral Armor

The Army is presently pursuing extensive combat readiness changes that include introducing a lightweight armored force. Consequently, development of lightweight armor solutions is at the forefront of attention. Among the potential solutions is a multifunctional polymer-matrix composite (PMC) composed of glass-fiber composite, ceramic, metal, and rubber. This PMC solution is termed "composite integral armor" (CIA) and allows the Army to combine mission-critical vehicle requirements into a single unified structure. The complex nature of the proposed armor solution for ground vehicles necessitates field-expedient and depot-level repair procedures for these thick-section components. A cross section of CIA is shown in Figure 27. This solution demonstrates the use of a seven-layer construction to provide unique ballistic and structural properties, multi-hit capability, flame protection, and signature management [20]. The surface composite layer protects the ceramics from surface damage and provides confinement. The ceramic strike face is built as an array of ceramic tiles supported by a composite backing plate (inner shell); together they contribute to the structural and ballistic properties of the armor. A nonlinear rubber layer separates the ceramic strike face and composite backing plate and increases the damage tolerance of the structure [21–24]. As well as advancements in ballistic and structural performance, requirements for combat vehicles incorporating CIA include provisions for maintenance and repair [25].

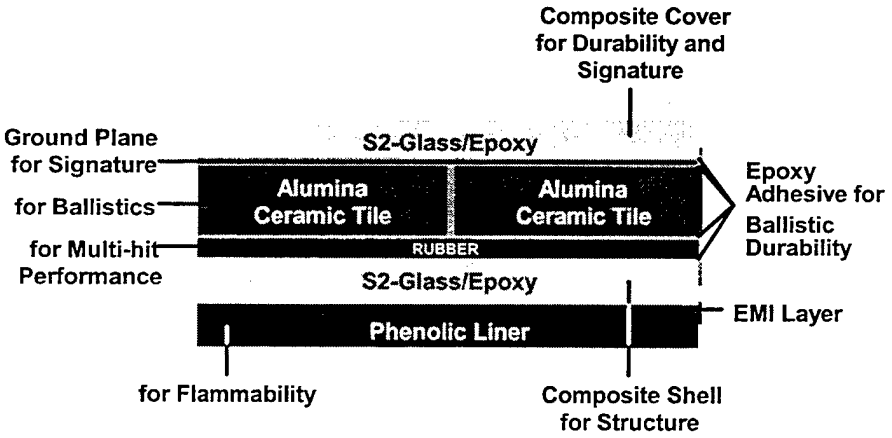

Figure 27. Multifunctional composite armor.

Conventional approaches for repair of composites (e.g., heat blankets, infrared heaters, and room-temperature paste adhesives) are surface-induced heating methods that are ineffective for repair of thick-section structures. For instance, heat blankets are effective only for processing less than 10 layers of carbon-fiber thermoset in aerospace applications due to thermal gradient impacts on resin performance [26]. Consequently, traditional repair of CIA will require adhesive bonding of a single layer at a time using a heat blanket, producing long processing times and increasing the exposure of the soldier to hazardous materials. Through-thickness curing approaches, such as E-beam curing, provide localized heating, enabling adhesive bonding for several layers (or even all layers) at once and reducing hazardous waste, energy consumption, and repair time.

Future experiments are scheduled to attempt an E-beam-processed repair of an integral armor panel. We will introduce a paste adhesive at each interface of the integral armor construct and perform both single and multistep cure processes for the armor system. It has been demonstrated by preliminary research that the extent of damage in the panel backing-plate is also significant on ballistic protection of the integral armor. Consequently, we anticipate the use of VARTM combined with E-beam curing will also be used to attempt back-plate repair. A restored panel will be tested ballistically to determine performance of the selected E-beam repair scheme.

3.2 Aircraft Skin Repair

Damage mechanisms for aircraft composite components include impact from bird strike, foreign object damage (FOD), ballistic impact, moisture intrusion and expansion, maintenance, and corrosion [27, 28]. Assessed damage levels in aircraft structures are classified according to severity and repairability as (1) light damage—aesthetic, surface or coating repair; (2) moderate damage—delaminations, non-structural patches, and edge repair; and (3) heavy damage—full depth, core and substructure repair. Other criteria for selecting the appropriate repair procedure include whether the component can be removed and whether the back side is accessible. A typical moderate repair is one-sided damage to the skin and underlying honeycomb core (Figure 28). Any remaining coating in the repair area is removed by hand sanding or portable tools. Damage is machined out in an appropriate configuration, often circular or racetrack. Scarfing, i.e., removal of skin material at a shallow angle, is commonly accomplished by hand, as automatic scarf routers are still under development and require additional refinement to be practical for most curved surface repair. Preparation of the repair surface for adhesive bonding includes wiping with solvent followed by grit blasting and compressed air brushing. A plug of honeycomb core replaces the damaged material. A skin patch is often partially cured off the aircraft using a double vacuum-bag cure [26]. The consolidated patch is then bonded to the aircraft using a qualified film adhesive and a heat blanket.

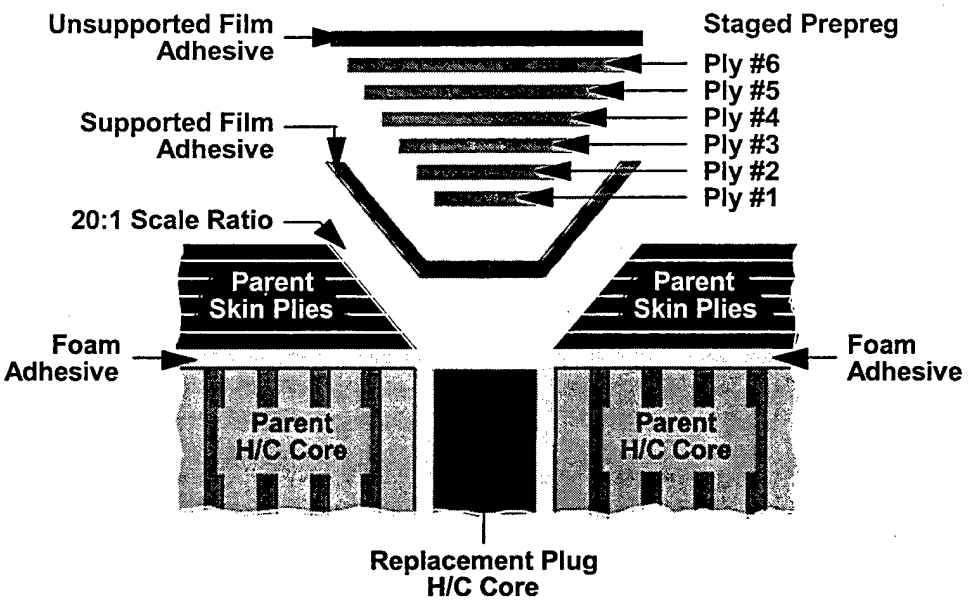

Figure 28. One-sided skin and honeycomb core repair.

We anticipate that E-beam processing will provide a novel and efficient method of obtaining rapid repair on aircraft surface structures. The ability to deliver energy for cure directly into the damage zone will allow on-aircraft repair to be achieved more efficiently. Currently, Air Canada has approved the use of E-beam adhesives for secondary structural repair of aircraft for commercial applications. The E-beam repaired demonstration systems produced by Air Canada and cured by Acsion Industries have equalled the repair quality and endurance of traditional thermal cure repair systems.

3.3 Military Airframe Remanufacture

Primary structure in an aircraft is a critical area of repair that has suffered due to limitations of thermal-cured repair systems available at this time. The need to achieve high temperatures for cure of film adhesives creates substantial limitations to repair of wing and spar sections of most military and commercial airframes. E-beam cure technology could provide an alternative to high-temperature cure cycles by providing high adhesives performance with low-temperature processing. Consequently, Northrop Grumman* has proposed an ideal airframe candidate, a cargo access panel, to demonstrate repair of primary, secondary and skin structures common to military aircraft systems. A typical access panel for the Joint Strike Fighter is shown in Figure 29. This panel possesses many of the unique aircraft structural elements including thin-section carbon-fiber composite, hat stiffeners, and angle-ply construction. The candidate

* 1 Hornet Way, El Segundo, CA 90245-2804.

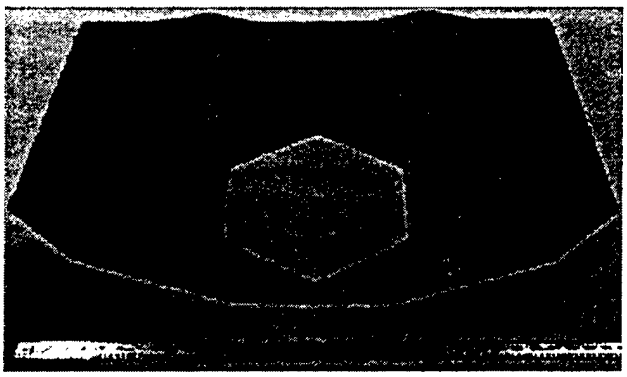

Figure 29. Composite airframe access panel from the Joint Strike Fighter development program.

part includes two integrally bonded hat stiffeners that provide increased stiffness for durability. We will fabricate a panel using an E-beam-processible VARTM resin to wet-out an AS4 carbon fiber preform. The fabricated article will be cured with E-beam irradiation.

In addition to fabricating this access panel, we will simulate damage in the panel by drilling or cutting out critical segments and demonstrate the repair of skin sections and hat-stiffeners using an E-beam-cured film adhesive and E-beam-curable prepreg patch that is consolidated using the double vacuum bag debulk technique.

Although traditional fabrication of all aircraft components involves prepreg consolidation and cure in an autoclave, we will demonstrate the feasibility of alternative processing by preparing this article with low-cost VARTM processing. Although manufacture of these small components using autoclave curing is reasonable, the small size of these components and the small area of repair make processing in an autoclave an environmentally costly approach. In repair, only a small single item is processed under special cure conditions for the adhesives. An autoclave with a volume capacity of more than 200 times the part volume is common, which results in large excesses in nitrogen oxides production during the curing stage of repair. Eliminating autoclave processing can dramatically decrease both the processing time and expense (environmental and economical) for these repairs. Both cationic and free-radical E-beam-cured materials will be used in the fabrication and repair of the demonstration article.

4. Conclusions

Ten years ago, the composites industry began investigating alternative cure technologies for high performance structures. Much of the initial development of electron beam curing of resins for composite applications was initiated in the

European community, and quickly became an approach sought by the aerospace and aircraft community. For example, the U.S. Air Force has invested significantly in building a materials database of radiation-cured resin systems, in hopes of reducing production costs and pollution impact of composite manufacturing.

After 10 years of development, many of the fundamental questions regarding cure by E-beam irradiation are still unanswered, although many resin systems have become available for low-performance applications. However, the aircraft industry continues to demand improvements in material properties, which results in occassional step increases in composite performance by E-beam irradiation curing.

In this report, the Army joins the crusade for improved low-cost resin systems for military applications. Part of the advantage to Army involvement in this technology development is a reduction of performance requirements. The Army is not pursuing the flightworthy E-beam-processed composite structures. As the Army strives to achieve a reduced logistic footprint and lightweight armored fighting force, composite structures for ground vehicle and ammunition applications become critical driving components of the technology. Here, we investigate the performance of traditional E-beam-cured resin systems, such as cationically cured epoxides and free-radical-cured acrylics and evaluate the performance of resins and composites fabricated from these systems. As our target performance parameters are much more generous that the aerospace industry, the feasibility of these materials coming into applications is greatly enhanced. However, vast improvements in both technological comprehension of the materials, as well as the performance of resin systems for Army applications are reported.

Particularly, a new approach to resin development is presented, where IPNs are used to achieve low-viscosity resins for VARTM molding of composite structures. Because traditional aerospace materials, such as composite prepreg, are designed for autoclave processing, achieving high performance in prepreg using only vacuum pressure is unlikely. However, VARTM processing provides a unique opportunity to develop excellent components with performance resins by looking at the fabrication of large composite structures from a low-cost approach. VARTM-type resins are now producing performance metrics for E-beam-cured composite structures that exceed traditional thermal-cured vinyl-ester performance capability. Therefore, utilization of E-beam as a processing method for composite ground vehicles continues to be a viable technological leap.

Additionally, E-beam-cured resin systems provide an opportunity to achieve performance of a vinyl-ester system but with a reduced environmental impact. The new technology formulations have low emission of volatile organic compounds and hazardous ozone depleting substances, because these new

systems are cured out-of-autoclave and do not possess highly volatile monomer units, such as styrene. Therefore, the success of this report can be partially understood by the environmental advantages that E-beam cure technology affords.

A final area of technology presented in this report is the development of adhesives for bonding applications. Clearly, a highly composites-based combat unit will have significant needs for repairability of mission critical units that are damaged in the field. E-beam technology affords an opportunity to develop materials for field cure environments, and E-beam adhesives are key to the success of depot-level repair demonstrations. A number of E-beam-cured adhesives have been demonstrated, including two-stage systems that cure by both room temperature and E-beam irradation methods. These two-stage adhesives provide technology for holding components together under ambient conditions prior to inducing cure with an E-beam curtain. Also, true E-beam adhesives that are consolidated under light heat and pressure have been demonstrated to provide reasonable failure strength in lap shear. The further development of these technologies is key to developing a lightweight and sustainable military force.

In summary, the technology available for E-beam processing of composite and adhesive structures has been investigated and new technology has been demonstrated to achieve performance requirements for ground vehicle applications for Army systems. Additional developments will be necessary in order to achieve "flightworthy" composite materials, but the Army has effectively demonstrated the ability to formulate resin compounds to meet weight and environmental restrictions for composite manufacture and repair of many proposed military vehicles.

5. References

1. Goodman, D. L., and G. R. Palmese. "Method of Making Fiber Reinforced Composites for Coatings." U.S. Patent 5,891,292, 1999.

2. Palmese, G. R., C. A. Byrne, and D. L. Goodman. "Advanced Electron Beam Curing System and Recent Composite Armored Vehicle Results." *SAMPE Proceedings*, vol. 42, no. 1, 1997.

3. Sands, J. M., S. H. McKnight, and B. K. Fink. "Formulation of Toughened Paste Adhesives for Reduced-Pollutant Electron Beam Repair and Assembly of Composite Structure." ARL-TR-2270, U.S. Army Research Laboratory, Aberdeen Proving Ground, MD, September 2000.

4. Sands, J. M., S. H. McKnight, and B. K. Fink. "Interpenetrating Polymer Network (IPN) Adhesives for Electron Beam Cure." ARL-TR-2321, U.S. Army Research Laboratory, Aberdeen Proving Ground, MD, September 2000.

5. Sands, J. M., S. H. McKnight, and B. K. Fink. "Nonpolluting Composites Repair and Remanufacturing for Military Applications: Formulation of Electron-Beam-Curable Resins With Enhanced Toughening." ARL-TR-2266, U.S. Army Research Laboratory, Aberdeen Proving Ground, MD, July 2000.

6. Sands, J. M., S. H. McKnight, R. Jensen, and K. Kit. "Experimental Preparation of Novel Sequential Interpenetrating Polymer Network Resins for Cure by Electron Beam Dose." *Journal of Applied Polymer Science*, vol. 81, pp. 530–545, 2001.

7. American Society for Testing and Materials. "Standard Test Methods for Flexural Properties of Unreinforced and Reinforced Plastics and Electrical Insulating Materials." ASTM D790-96a, American Society for Testing and Materials Electronic Media, 1999.

8. American Society for Testing and Materials. "Standard Test Methods for Plane-Strain Fracture Toughness and Strain Energy Release Rate of Plastic Materials." ASTM D5045-93, American Society for Testing and Materials Electronic Media, 1999.

9. Sung, P. H., and C. Y. Lin. "Polysiloxane Modified Epoxy Polymer Network II. Dynamic Mechanical Behavior of Multicomponent Graft-IPNs (Epoxy/Polysiloxane/Polypropylene Glycol)." *European Polymer Journal*, vol. 33, p. 231, 1997.

10. Tang, H., L. Dong, J. Zhang, M. Ding, and Z. Feng. "Miscibility and Crystalization Behavior of Thermosetting Polyimide/Thermoplastic Polyimide Blends." *Macromolecular Chemistry and Physics*, vol. 197, no. 2, p. 543, 1996.

11. Li, Y., and S. Mao. "A Study on the Glass Transition Behavior and Morphology of Semi-Interpenetrating Polymer Networks." *Journal of Polymer Science: Polymer Chemistry*, vol. 34, p. 2371, 1996.

12. Bartolotta, A., G. Di Marco, G. Carini, G. D'Angelo, G. Tripodo, A. M. Fainleib, E. A. Slinchenko, V. I. Shtompel, and V. P. Privalko. "Synthesis and Physical Characterization of Semi-IPNs of Linear Polyurethane and Heterocyclic Polymer Networks." *Polymer Engineering and Science*, vol. 39, p. 549, 1999.

13. Aklonis, J. J., and W. J. MacKnight. *Introduction to Polymer Viscoelasticity.* Second edition, New York: John Wiley and Sons, 1983.

14. American Society for Testing and Materials. "Standard Test Method for Tensile Properties of Polymer Matrix Composites Materials." ASTM D3039/D3039M-95a, American Society for Testing and Materials Electronic Media, 1999.

15. American Society for Testing and Materials. "Standard Test Method for Compressing Properties of Polymer Matrix Composite Materials with Unsupported Gage Section by Shear Loading." ASTM D3410/D3410M-95, American Society for Testing and Materials Electronic Media, 1999.

16. American Society for Testing and Materials. "Standard Test Method for Shear Properties of Composite Materials by the V-Notched Beam Method." ASTM D5379/D5379M-98, American Society for Testing and Materials Electronic Media, 1999.

17. Palmese, G. R., N. N. Ghosh, and S. H. McKnight. "Investigation of Factors Influencing the Cationic Polymerization of Epoxy Resins." *SAMPE Proceedings*, vol. 45, p. 2188, 2000.

18. American Society for Testing and Materials. "Standard Test Method for Apparent Interlaminar Shear Strength of Parallel Fiber Composites by Short-Beam Method." ASTM D2344-84, American Society for Testing and Materials Electronic Media, 1999.

19. Defoort, B., and L. T. Drzal. "Adhesion Between Carbon Fibers and Cationic Matrices in Electron Beam Processed Composites." *SAMPE Proceedings*, vol. 47, p. 2063, 2001.

20. Gama, B. A., T. A. Bogetti, B. K. Fink, and J. W. Gillespie Jr. "Processing, Ballistic Testing and Repair of Composite Integral Armor." Proceedings of the 32nd International SAMPE Technical Conference, Boston, MA, 5–9 November 2000.

21. United Defense Limited Partnership. "Design Guide, Composite Armored Vehicle Advanced Technology Demonstrator (CAV-ATD)." Arlington, VA, April 1998.

22. Fink, B. K., and J. W. Gillespie, Jr. "Cost-Effective Manufacturing of Damage Tolerant Integral Armor." ARL-TR-2319, U.S. Army Research Laboratory, Aberdeen Proving Ground, MD, September 2000.

23. Monib, A. M., J. W. Gillespie, Jr., and B. K. Fink. "Damage Tolerance of Thick-Section Composites Subjected to Ballistic Impact." CCM Report No. 99-08, University of Delaware, Newark, DE, 1999.

24. Gama, B. A., J. W. Gillespie, Jr., H. Mahfuz, T. A. Bogetti, and B. K. Fink. "Effect of Non-Linear Material Behavior on the Through-Thickness Stress Wave Propagation in Multi-Layer Hybrid Lightweight Armor." International Conference on Computational Engineering and Sciences, Los Angeles, CA, August 2000.

25. Fink, B. K. "Performance Metrics for Composite Integral Armor." *Journal of Thermoplastic Composite Materials*, vol. 13, pp. 417–431, September 2000.

26. Clements, H., and P. Mehrkam. "Development of the Navy Double Vacuum Debulk Process." DOD Composite Repair Workshop V, Coeur d'Alene, ID, 13–16 November 2000.

27. Mehrkam, P. "Support of Composite Structures on Naval Aircraft." Second Joint NASA/FAA/DOD Conference on Aging Aircraft, Williamsburg, VA, 31 August–3 September 1998.

28. Koon, R. W. "Aircraft Skin Repair Procedures and Requirements." Presented at the U.S. Army Research Laboratory, Aberdeen Proving Ground, MD, 24 August 1998.

INTENTIONALLY LEFT BLANK.

NO. OF COPIES	ORGANIZATION
2	DEFENSE TECHNICAL INFORMATION CENTER DTIC OCA 8725 JOHN J KINGMAN RD STE 0944 FT BELVOIR VA 22060-6218
1	HQDA DAMO FDT 400 ARMY PENTAGON WASHINGTON DC 20310-0460
1	OSD OUSD(A&T)/ODDR&E(R) DR R J TREW 3800 DEFENSE PENTAGON WASHINGTON DC 20301-3800
1	COMMANDING GENERAL US ARMY MATERIEL CMD AMCRDA TF 5001 EISENHOWER AVE ALEXANDRIA VA 22333-0001
1	INST FOR ADVNCD TCHNLGY THE UNIV OF TEXAS AT AUSTIN 3925 W BRAKER LN STE 400 AUSTIN TX 78759-5316
1	US MILITARY ACADEMY MATH SCI CTR EXCELLENCE MADN MATH THAYER HALL WEST POINT NY 10996-1786
1	DIRECTOR US ARMY RESEARCH LAB AMSRL D DR D SMITH 2800 POWDER MILL RD ADELPHI MD 20783-1197
1	DIRECTOR US ARMY RESEARCH LAB AMSRL CI AI R 2800 POWDER MILL RD ADELPHI MD 20783-1197

NO. OF COPIES	ORGANIZATION
3	DIRECTOR US ARMY RESEARCH LAB AMSRL CI LL 2800 POWDER MILL RD ADELPHI MD 20783-1197
3	DIRECTOR US ARMY RESEARCH LAB AMSRL CI IS T 2800 POWDER MILL RD ADELPHI MD 20783-1197
	ABERDEEN PROVING GROUND
2	DIR USARL AMSRL CI LP (BLDG 305)

NO. OF COPIES	ORGANIZATION
1	DIRECTOR US ARMY RESEARCH LAB AMSRL CP CA D SNIDER 2800 POWDER MILL RD ADELPHI MD 20783-1145
1	DIRECTOR US ARMY RESEARCH LAB AMSRL CI IS R 2800 POWDER MILL RD ADELPHI MD 20783-1145
3	DIRECTOR US ARMY RESEARCH LAB AMSRL OP SD TL 2800 POWDER MILL RD ADELPHI MD 20783-1145
1	DIRECTOR US ARMY RESEARCH LAB AMSRL CI IS T 2800 POWDER MILL RD ADELPHI MD 20783-1145
1	DIRECTOR DA OASARDA SARD SO 103 ARMY PENTAGON WASHINGTON DC 20310-0103
1	DPTY ASST SECY FOR R&T SARD TT THE PENTAGON RM 3EA79 WASHINGTON DC 20301-7100
1	COMMANDER US ARMY MATERIEL CMD AMXMI INT 5001 EISENHOWER AVE ALEXANDRIA VA 22333-0001
4	COMMANDER US ARMY ARDEC AMSTA AR CC G PAYNE J GEHBAUER C BAULIEU H OPAT PICATINNY ARSENAL NJ 07806-5000
2	COMMANDER US ARMY ARDEC AMSTA AR AE WW E BAKER J PEARSON PICATINNY ARSENAL NJ 07806-5000
1	COMMANDER US ARMY ARDEC AMSTA AR TD C SPINELLI PICATINNY ARSENAL NJ 07806-5000
1	COMMANDER US ARMY ARDEC AMSTA AR FSE PICATINNY ARSENAL NJ 07806-5000
6	COMMANDER US ARMY ARDEC AMSTA AR CCH A W ANDREWS S MUSALLI R CARR M LUCIANO E LOGSDEN T LOUZEIRO PICATINNY ARSENAL NJ 07806-5000
1	COMMANDER US ARMY ARDEC AMSTA AR CCH P J LUTZ PICATINNY ARSENAL NJ 07806-5000
1	COMMANDER US ARMY ARDEC AMSTA AR FSF T C LIVECCHIA PICATINNY ARSENAL NJ 07806-5000
1	COMMANDER US ARMY ARDEC AMSTA ASF PICATINNY ARSENAL NJ 07806-5000

NO. OF COPIES	ORGANIZATION
1	COMMANDER US ARMY ARDEC AMSTA AR QAC T C C PATEL PICATINNY ARSENAL NJ 07806-5000
1	COMMANDER US ARMY ARDEC AMSTA AR M D DEMELLA PICATINNY ARSENAL NJ 07806-5000
3	COMMANDER US ARMY ARDEC AMSTA AR FSA A WARNASH B MACHAK M CHIEFA PICATINNY ARSENAL NJ 07806-5000
2	COMMANDER US ARMY ARDEC AMSTA AR FSP G M SCHIKSNIS D CARLUCCI PICATINNY ARSENAL NJ 07806-5000
1	COMMANDER US ARMY ARDEC AMSTA AR FSP A P KISATSKY PICATINNY ARSENAL NJ 07806-5000
2	COMMANDER US ARMY ARDEC AMSTA AR CCH C H CHANIN S CHICO PICATINNY ARSENAL NJ 07806-5000
1	COMMANDER US ARMY ARDEC AMSTA AR QAC T D RIGOGLIOSO PICATINNY ARSENAL NJ 07806-5000

NO. OF COPIES	ORGANIZATION
1	COMMANDER US ARMY ARDEC AMSTA AR WET T SACHAR BLDG 172 PICATINNY ARSENAL NJ 07806-5000
9	COMMANDER US ARMY ARDEC AMSTA AR CCH B P DONADIA F DONLON P VALENTI C KNUTSON G EUSTICE S PATEL G WAGNECZ R SAYER F CHANG PICATINNY ARSENAL NJ 07806-5000
6	COMMANDER US ARMY ARDEC AMSTA AR CCL F PUZYCKI R MCHUGH D CONWAY E JAROSZEWSKI R SCHLENNER M CLUNE PICATINNY ARSENAL NJ 07806-5000
5	PM SADARM SFAE GCSS SD COL B ELLIS M DEVINE W DEMASSI J PRITCHARD S HROWNAK PICATINNY ARSENAL NJ 07806-5000
1	US ARMY ARDEC INTELLIGENCE SPECIALIST AMSTA AR WEL F M GUERRIERE PICATINNY ARSENAL NJ 07806-5000

NO. OF COPIES	ORGANIZATION
2	PEO FIELD ARTILLERY SYS SFAE FAS PM H GOLDMAN T MCWILLIAMS PICATINNY ARSENAL NJ 07806-5000
12	PM TMAS SFAE GSSC TMA R MORRIS C KIMKER D GUZIEWICZ E KOPACZ R ROESER R DARCY R KOWALSKI R MCDANOLDS L D ULISSE C ROLLER J MCGREEN B PATTER PICATINNY ARSENAL NJ 07806-5000
1	COMMANDER US ARMY ARDEC AMSTA AR WEA J BRESCIA PICATINNY ARSENAL NJ 07806-5000
1	COMMANDER US ARMY ARDEC PRODUCTION BASE MODERN ACTY AMSMC PBM K PICATINNY ARSENAL NJ 07806-5000
1	COMMANDER US ARMY TACOM PM ABRAMS SFAE ASM AB 6501 ELEVEN MILE RD WARREN MI 48397-5000
1	COMMANDER US ARMY TACOM AMSTA SF WARREN MI 48397-5000
1	COMMANDER US ARMY TACOM PM BFVS SFAE GCSS W BV 6501 ELEVEN MILE RD WARREN MI 48397-5000
1	DIRECTOR AIR FORCE RESEARCH LAB MLLMD D MIRACLE 2230 TENTH ST WRIGHT PATTERSON AFB OH 45433-7817
1	OFC OF NAVAL RESEARCH J CHRISTODOULOU ONR CODE 332 800 N QUINCY ST ARLINGTON VA 22217-5600
1	US ARMY CERL R LAMPO 2902 NEWMARK DR CHAMPAIGN IL 61822
1	COMMANDER US ARMY TACOM PM SURVIVABLE SYSTEMS SFAE GCSS W GSI H M RYZYI 6501 ELEVEN MILE RD WARREN MI 48397-5000
1	COMMANDER US ARMY TACOM CHIEF ABRAMS TESTING SFAE GCSS W AB QT T KRASKIEWICZ 6501 ELEVEN MILE RD WARREN MI 48397-5000
1	COMMANDER WATERVLIET ARSENAL SMCWV QAE Q B VANINA BLDG 44 WATERVLIET NY 12189-4050

NO. OF COPIES	ORGANIZATION
3	ARMOR SCHOOL ATZK TD R BAUEN J BERG A POMEY FT KNOX KY 40121
14	COMMANDER US ARMY TACOM AMSTA TR R R MCCLELLAND D THOMAS J BENNETT D HANSEN AMSTA JSK S GOODMAN J FLORENCE K IYER D TEMPLETON A SCHUMACHER AMSTA TR D D OSTBERG L HINOJOSA B RAJU AMSTA CS SF H HUTCHINSON F SCHWARZ WARREN MI 48397-5000
14	BENET LABORATORIES AMSTA AR CCB R FISCELLA M SOJA E KATHE M SCAVULO G SPENCER P WHEELER S KRUPSKI J VASILAKIS G FRIAR R HASENBEIN AMSTA CCB R S SOPOK E HYLAND D CRAYON R DILLON WATERVLIET NY 12189-4050

NO. OF COPIES	ORGANIZATION
2	HQ IOC TANK AMMUNITION TEAM AMSIO SMT R CRAWFORD W HARRIS ROCK ISLAND IL 61299-6000
2	COMMANDER US ARMY AMCOM AVIATION APPLIED TECH DIR J SCHUCK FT EUSTIS VA 23604-5577
1	DIRECTOR US ARMY AMCOM SFAE AV RAM TV D CALDWELL BLDG 5300 REDSTONE ARSENAL AL 35898
2	US ARMY CORPS OF ENGINEERS CERD C T LIU CEW ET T TAN 20 MASS AVE NW WASHINGTON DC 20314
1	US ARMY COLD REGIONS RSCH & ENGRNG LAB P DUTTA 72 LYME RD HANOVER NH 03755
1	USA SBCCOM PM SOLDIER SPT AMSSB PM RSS A J CONNORS KANSAS ST NATICK MA 01760-5057
2	USA SBCCOM MATERIAL SCIENCE TEAM AMSSB RSS J HERBERT M SENNETT KANSAS ST NATICK MA 01760-5057

NO. OF COPIES	ORGANIZATION
2	OFC OF NAVAL RESEARCH D SIEGEL CODE 351 J KELLY 800 N QUINCY ST ARLINGTON VA 22217-5660
1	NAVAL SURFACE WARFARE CTR DAHLGREN DIV CODE G06 DAHLGREN VA 22448
1	NAVAL SURFACE WARFARE CTR TECH LIBRARY CODE 323 17320 DAHLGREN RD DAHLGREN VA 22448
1	NAVAL SURFACE WARFARE CTR CRANE DIVISION M JOHNSON CODE 20H4 LOUISVILLE KY 40214-5245
2	NAVAL SURFACE WARFARE CTR U SORATHIA C WILLIAMS CD 6551 9500 MACARTHUR BLVD WEST BETHESDA MD 20817
2	COMMANDER NAVAL SURFACE WARFARE CTR CARDEROCK DIVISION R PETERSON CODE 2020 M CRITCHFIELD CODE 1730 BETHESDA MD 20084
8	DIRECTOR US ARMY NATIONAL GROUND INTELLIGENCE CTR D LEITER M HOLTUS M WOLFE S MINGLEDORF J GASTON W GSTATTENBAUER R WARNER J CRIDER 220 SEVENTH ST NE CHARLOTTESVILLE VA 22091
8	US ARMY SBCCOM SOLDIER SYSTEMS CENTER BALLISTICS TEAM J WARD W ZUKAS P CUNNIFF J SONG MARINE CORPS TEAM J MACKIEWICZ BUS AREA ADVOCACY TEAM W HASKELL AMSSB RCP SS W NYKVIST S BEAUDOIN KANSAS ST NATICK MA 01760-5019
9	US ARMY RESEARCH OFC A CROWSON H EVERETT J PRATER G ANDERSON D STEPP D KISEROW J CHANG PO BOX 12211 RESEARCH TRIANGLE PARK NC 27709-2211
1	NAVAL SEA SYSTEMS CMD D LIESE 2531 JEFFERSON DAVIS HWY ARLINGTON VA 22242-5160
1	NAVAL SURFACE WARFARE CTR M LACY CODE B02 17320 DAHLGREN RD DAHLGREN VA 22448
8	NAVAL SURFACE WARFARE CTR J FRANCIS CODE G30 D WILSON CODE G32 R D COOPER CODE G32 J FRAYSSE CODE G33 E ROWE CODE G33 T DURAN CODE G33 L DE SIMONE CODE G33 R HUBBARD CODE G33 DAHLGREN VA 22448

NO. OF COPIES	ORGANIZATION
2	NAVAL SURFACE WARFARE CTR CARDEROCK DIVISION R CRANE CODE 2802 C WILLIAMS CODE 6553 3A LEGGETT CIR BETHESDA MD 20054-5000
1	EXPEDITIONARY WARFARE DIV N85 F SHOUP 2000 NAVY PENTAGON WASHINGTON DC 20350-2000
1	AFRL MLBC 2941 P ST RM 136 WRIGHT PATTERSON AFB OH 45433-7750
1	AFRL MLSS R THOMSON 2179 12TH ST RM 122 WRIGHT PATTERSON AFB OH 45433-7718
2	AFRL F ABRAMS J BROWN BLDG 653 2977 P ST STE 6 WRIGHT PATTERSON AFB OH 45433-7739
1	WATERWAYS EXPERIMENT D SCOTT 3909 HALLS FERRY RD SC C VICKSBURG MS 39180
5	DIRECTOR LLNL R CHRISTENSEN S DETERESA F MAGNESS M FINGER MS 313 M MURPHY L 282 PO BOX 808 LIVERMORE CA 94550
1	AFRL MLS OL L COULTER 7278 4TH ST BLDG 100 BAY D HILL AFB UT 84056-5205

NO. OF COPIES	ORGANIZATION
1	OSD JOINT CCD TEST FORCE OSD JCCD R WILLIAMS 3909 HALLS FERRY RD VICKSBURG MS 29180-6199
3	DARPA M VANFOSSEN S WAX L CHRISTODOULOU 3701 N FAIRFAX DR ARLINGTON VA 22203-1714
2	SERDP PROGRAM OFC PM P2 C PELLERIN B SMITH 901 N STUART ST STE 303 ARLINGTON VA 22203
1	FAA MIL HDBK 17 CHAIR L ILCEWICZ 1601 LIND AVE SW ANM 115N RESTON VA 98055
1	US DEPT OF ENERGY OFC OF ENVIRONMENTAL MANAGEMENT P RITZCOVAN 19901 GERMANTOWN RD GERMANTOWN MD 20874-1928
1	DIRECTOR LOS ALAMOS NATIONAL LAB F L ADDESSIO T 3 MS 5000 PO BOX 1633 LOS ALAMOS NM 87545
1	OAK RIDGE NATIONAL LABORATORY R M DAVIS PO BOX 2008 OAK RIDGE TN 37831-6195
1	OAK RIDGE NATIONAL LABORATORY C EBERLE MS 8048 PO BOX 2008 OAK RIDGE TN 37831

NO. OF COPIES	ORGANIZATION
3	DIRECTOR SANDIA NATIONAL LABS APPLIED MECHANICS DEPT MS 9042 J HANDROCK Y R KAN J LAUFFER PO BOX 969 LIVERMORE CA 94551-0969
1	OAK RIDGE NATIONAL LABORATORY C D WARREN MS 8039 PO BOX 2008 OAK RIDGE TN 37831
5	NIST J DUNKERS M VANLANDINGHAM MS 8621 J CHIN MS 8621 J MARTIN MS 8621 D DUTHINH MS 8611 100 BUREAU DR GAITHERSBURG MD 20899
1	HYDROGEOLOGIC INC SERDP ESTCP SPT OFC S WALSH 1155 HERNDON PKWY STE 900 HERNDON VA 20170
3	NASA LANGLEY RSCH CTR AMSRL VS W ELBER MS 266 F BARTLETT JR MS 266 G FARLEY MS 266 HAMPTON VA 23681-0001
1	NASA LANGLEY RSCH CTR T GATES MS 188E HAMPTON VA 23661-3400
1	FHWA E MUNLEY 6300 GEORGETOWN PIKE MCLEAN VA 22101
1	USDOT FEDERAL RAILRD M FATEH RDV 31 WASHINGTON DC 20590

NO. OF COPIES	ORGANIZATION
3	CYTEC FIBERITE R DUNNE D KOHLI R MAYHEW 1300 REVOLUTION ST HAVRE DE GRACE MD 21078
1	MARINE CORPS INTLLGNC ACTVTY D KOSITZKE 3300 RUSSELL RD STE 250 QUANTICO VA 22134-5011
1	DIRECTOR NATIONAL GRND INTLLGNC CTR IANG TMT 220 SEVENTH ST NE CHARLOTTESVILLE VA 22902-5396
1	SIOUX MFG B KRIEL PO BOX 400 FT TOTTEN ND 58335
2	3TEX CORPORATION A BOGDANOVICH J SINGLETARY 109 MACKENAN DR CARY NC 27511
1	3M CORPORATION J SKILDUM 3M CENTER BLDG 60 IN 01 ST PAUL MN 55144-1000
1	DIRECTOR DEFENSE INTLLGNC AGNCY TA 5 K CRELLING WASHINGTON DC 20310
1	ADVANCED GLASS FIBER YARNS T COLLINS 281 SPRING RUN LANE STE A DOWNINGTON PA 19335
1	COMPOSITE MATERIALS INC D SHORTT 19105 63 AVE NE PO BOX 25 ARLINGTON WA 98223

NO. OF COPIES	ORGANIZATION
1	JPS GLASS L CARTER PO BOX 260 SLATER RD SLATER SC 29683
1	COMPOSITE MATERIALS INC R HOLLAND 11 JEWEL CT ORINDA CA 94563
1	COMPOSITE MATERIALS INC C RILEY 14530 S ANSON AVE SANTA FE SPRINGS CA 90670
2	SIMULA J COLTMAN R HUYETT 10016 S 51ST ST PHOENIX AZ 85044
2	PROTECTION MATERIALS INC M MILLER F CRILLEY 14000 NW 58 CT MIAMI LAKES FL 33014
2	FOSTER MILLER M ROYLANCE W ZUKAS 195 BEAR HILL RD WALTHAM MA 02354-1196
1	ROM DEVELOPMENT CORP R O MEARA 136 SWINEBURNE ROW BRICK MARKET PLACE NEWPORT RI 02840
2	TEXTRON SYSTEMS T FOLTZ M TREASURE 1449 MIDDLESEX ST LOWELL MA 01851
1	O GARA HESS & EISENHARDT M GILLESPIE 9113 LESAINT DR FAIRFIELD OH 45014

NO. OF COPIES	ORGANIZATION
2	MILLIKEN RSCH CORP H KUHN M MACLEOD PO BOX 1926 SPARTANBURG SC 29303
1	CONNEAUGHT INDUSTRIES INC J SANTOS PO BOX 1425 COVENTRY RI 02816
1	BATTELLE NATICK OPNS B HALPIN 209 W CENTRAL ST STE 302 NATICK MA 01760
1	ARMTEC DEFENSE PRODUCTS S DYER 85 901 AVE 53 PO BOX 848 COACHELLA CA 92236
1	NATIONAL COMPOSITE CENTER T CORDELL 2000 COMPOSITE DR KETTERING OH 45420
3	PACIFIC NORTHWEST LAB M SMITH G VAN ARSDALE R SHIPPELL PO BOX 999 RICHLAND WA 99352
2	AMOCO PERFORMANCE PRODUCTS M MICHNO JR J BANISAUKAS 4500 MCGINNIS FERRY RD ALPHARETTA GA 30202-3944
8	ALLIANT TECHSYSTEMS INC C CANDLAND MN11 2830 C AAKHUS MN11 2830 B SEE MN11 2439 N VLAHAKUS MN11 2145 R DOHRN MN11 2830 S HAGLUND MN11 2439 M HISSONG MN11 2830 D KAMDAR MN11 2830 600 SECOND ST NE HOPKINS MN 55343-8367

NO. OF COPIES	ORGANIZATION
1	SAIC M PALMER 1410 SPRING HILL RD STE 400 MS SH4 5 MCLEAN VA 22102
1	SAIC G CHRYSSOMALLIS 3800 W 80TH ST STE 1090 BLOOMINGTON MN 55431
1	AAI CORPORATION T G STASTNY PO BOX 126 HUNT VALLEY MD 21030-0126
1	APPLIED COMPOSITES W GRISCH 333 NORTH SIXTH ST ST CHARLES IL 60174
1	CUSTOM ANALYTICAL ENG SYS INC A ALEXANDER 13000 TENSOR LANE NE FLINTSTONE MD 21530
3	ALLIANT TECHSYSTEMS INC J CONDON E LYNAM J GERHARD WV01 16 STATE RT 956 PO BOX 210 ROCKET CENTER WV 26726-0210
1	OFC DEPUTY UNDER SEC DEFNS J THOMPSON 1745 JEFFERSON DAVIS HWY CRYSTAL SQ 4 STE 501 ARLINGTON VA 22202
1	PROJECTILE TECHNOLOGY INC 515 GILES ST HAVRE DE GRACE MD 21078
3	HEXCEL INC R BOE PO BOX 18748 SALT LAKE CITY UT 84118
5	AEROJET GEN CORP D PILLASCH T COULTER C FLYNN D RUBAREZUL M GREINER 1100 WEST HOLLYVALE ST AZUSA CA 91702-0296
1	HERCULES INC HERCULES PLAZA WILMINGTON DE 19894
1	BRIGS COMPANY J BACKOFEN 2668 PETERBOROUGH ST HERNDON VA 22071-2443
1	ZERNOW TECHNICAL SERVICES L ZERNOW 425 W BONITA AVE STE 208 SAN DIMAS CA 91773
1	GENERAL DYNAMICS OTS L WHITMORE 10101 NINTH ST NORTH ST PETERSBURG FL 33702
3	GENERAL DYNAMICS OTS FLINCHBAUGH DIV E STEINER B STEWART T LYNCH PO BOX 127 RED LION PA 17356
1	GKN AEROSPACE D OLDS 15 STERLING DR WALLINGFORD CT 06492
5	SIKORSKY AIRCRAFT G JACARUSO T CARSTENSAN B KAY S GARBO MS S330A J ADELMANN 6900 MAIN ST PO BOX 9729 STRATFORD CT 06497-9729

NO. OF COPIES	ORGANIZATION
1	PRATT & WHITNEY C WATSON 400 MAIN ST MS 114 37 EAST HARTFORD CT 06108
1	AEROSPACE CORP G HAWKINS M4 945 2350 E EL SEGUNDO BLVD EL SEGUNDO CA 90245
2	CYTEC FIBERITE M LIN W WEB 1440 N KRAEMER BLVD ANAHEIM CA 92806
1	UDLP G THOMAS PO BOX 58123 SANTA CLARA CA 95052
2	UDLP R BARRETT MAIL DROP M53 V HORVATICH MAIL DROP M53 328 W BROKAW RD SANTA CLARA CA 95052-0359
3	UDLP GROUND SYSTEMS DIVISION M PEDRAZZI MAIL DROP N09 A LEE MAIL DROP N11 M MACLEAN MAIL DROP N06 1205 COLEMAN AVE SANTA CLARA CA 95052
4	UDLP R BRYNSVOLD P JANKE MS 170 4800 EAST RIVER RD MINNEAPOLIS MN 55421-1498
2	BOEING DFNSE & SPACE GP W HAMMOND S 4X55 J RUSSELL S 4X55 PO BOX 3707 SEATTLE WA 98124-2207
2	BOEING ROTORCRAFT P MINGURT P HANDEL 800 B PUTNAM BLVD WALLINGFORD PA 19086

NO. OF COPIES	ORGANIZATION
1	BOEING DOUGLAS PRODUCTS DIV L J HART SMITH 3855 LAKEWOOD BLVD D800 0019 LONG BEACH CA 90846-0001
1	LOCKHEED MARTIN SKUNK WORKS D FORTNEY 1011 LOCKHEED WAY PALMDALE CA 93599-2502
1	LOCKHEED MARTIN R FIELDS 1195 IRWIN CT WINTER SPRINGS FL 32708
1	MATERIALS SCIENCES CORP G FLANAGAN 500 OFC CENTER DR STE 250 FT WASHINGTON PA 19034
1	NORTHRUP GRUMMAN CORP ELECTRONIC SENSORS & SYSTEMS DIV E SCHOCH MS V 16 1745A W NURSERY RD LINTHICUM MD 21090
1	GDLS DIVISION D BARTLE PO BOX 1901 WARREN MI 48090
2	GDLS D REES M PASIK PO BOX 2074 WARREN MI 48090-2074
1	GDLS MUSKEGON OPERATIONS W SOMMERS JR 76 GETTY ST MUSKEGON MI 49442
1	GENERAL DYNAMICS AMPHIBIOUS SYS SURVIVABILITY LEAD G WALKER 991 ANNAPOLIS WAY WOODBRIDGE VA 22191

NO. OF COPIES	ORGANIZATION
6	INST FOR ADVANCED TECH H FAIR I MCNAB P SULLIVAN S BLESS W REINECKE C PERSAD 3925 W BRAKER LN STE 400 AUSTIN TX 78759-5316
2	CIVIL ENGR RSCH FOUNDATION PRESIDENT H BERNSTEIN R BELLE 1015 15TH ST NW STE 600 WASHINGTON DC 20005
1	ARROW TECH ASSO 1233 SHELBURNE RD STE D8 SOUTH BURLINGTON VT 05403-7700
1	R EICHELBERGER CONSULTANT 409 W CATHERINE ST BEL AIR MD 21014-3613
1	UCLA MANE DEPT ENGR IV H T HAHN LOS ANGELES CA 90024-1597
2	UNIV OF DAYTON RESEARCH INST R Y KIM A K ROY 300 COLLEGE PARK AVE DAYTON OH 45469-0168
1	UMASS LOWELL PLASTICS DEPT N SCHOTT 1 UNIVERSITY AVE LOWELL MA 01854
1	IIT RESEARCH CENTER D ROSE 201 MILL ST ROME NY 13440-6916

NO. OF COPIES	ORGANIZATION
1	GA TECH RSCH INST GA INST OF TCHNLGY P FRIEDERICH ATLANTA GA 30392
1	MICHIGAN ST UNIV MSM DEPT R AVERILL 3515 EB EAST LANSING MI 48824-1226
1	UNIV OF WYOMING D ADAMS PO BOX 3295 LARAMIE WY 82071
2	PENN STATE UNIV R MCNITT C BAKIS 212 EARTH ENGR SCIENCES BLDG UNIVERSITY PARK PA 16802
1	PENN STATE UNIV R S ENGEL 245 HAMMOND BLDG UNIVERSITY PARK PA 16801
1	PURDUE UNIV SCHOOL OF AERO & ASTRO C T SUN W LAFAYETTE IN 47907-1282
1	STANFORD UNIV DEPT OF AERONAUTICS & AEROBALLISTICS S TSAI DURANT BLDG STANFORD CA 94305
1	UNIV OF MAIN ADV STR & COMP LAB R LOPEZ ANIDO 5793 AEWC BLDG ORONO ME 04469-5793
1	JOHNS HOPKINS UNIV APPLIED PHYSICS LAB P WIENHOLD 11100 JOHNS HOPKINS RD LAUREL MD 20723-6099

NO. OF COPIES	ORGANIZATION
1	UNIV OF DAYTON J M WHITNEY COLLEGE PARK AVE DAYTON OH 45469-0240
5	UNIV OF DELAWARE CTR FOR COMPOSITE MTRLS J GILLESPIE M SANTARE S YARLAGADDA S ADVANI D HEIDER 201 SPENCER LABORATORY NEWARK DE 19716
1	DEPT OF MATERIALS SCIENCE & ENGINEERING UNIVERSITY OF ILLINOIS AT URBANA CHAMPAIGN J ECONOMY 1304 WEST GREEN ST 115B URBANA IL 61801
1	NORTH CAROLINA STATE UNIV CIVIL ENGINEERING DEPT W RASDORF PO BOX 7908 RALEIGH NC 27696-7908
1	UNIV OF MARYLAND DEPT OF AEROSPACE ENGNRNG A J VIZZINI COLLEGE PARK MD 20742
3	UNIV OF TEXAS AT AUSTIN CTR FOR ELECTROMECHANICS J PRICE A WALLS J KITZMILLER 10100 BURNET RD AUSTIN TX 78758-4497
1	DREXEL UNIV A S D WANG 32ND & CHESTNUT ST PHILADELPHIA PA 19104
3	VA POLYTECHNICAL INST & STATE UNIV DEPT OF ESM M W HYER K REIFSNIDER R JONES BLACKSBURG VA 24061-0219
1	SOUTHWEST RSCH INST ENGR & MATL SCIENCES DIV J RIEGEL 6220 CULEBRA RD PO DRAWER 28510 SAN ANTONIO TX 78228-0510
	ABERDEEN PROVING GROUND
1	US ARMY MATERIEL SYSTEMS ANALYSIS ACTIVITY P DIETZ 392 HOPKINS RD AMXSY TD APG MD 21005-5071
1	DIRECTOR US ARMY RESEARCH LAB AMSRL OP AP L APG MD 21005-5066
90	DIR USARL AMSRL CI AMSRL CI S A MARK AMSRL CS IO FI M ADAMSON AMSRL SL BA AMSRL SL BL D BELY R HENRY AMSRL SL BG AMSRL SL I AMSRL WM J SMITH AMSRL WM B A HORST AMSRL WM BA D LYON

NO. OF
COPIES ORGANIZATION

ABERDEEN PROVING GROUND (CONT)

AMSRL WM BC
P PLOSTINS
J NEWILL
S WILKERSON
A ZIELINSKI
AMSRL WM BD
B FORCH
R FIFER
R PESCE RODRIGUEZ
B RICE
AMSRL WM BE
C LEVERITT
AMSRL WM BF
J LACETERA
AMSRL WM BR
C SHOEMAKER
J BORNSTEIN
AMSRL WM M
D VIECHNICKI
G HAGNAUER
J MCCAULEY
AMSRL WM MA
L GHIORSE
S MCKNIGHT
AMSRL WM MB
B FINK
J BENDER
T BOGETTI
R BOSSOLI
L BURTON
K BOYD
S CORNELISON
P DEHMER
R DOOLEY
W DRYSDALE
G GAZONAS
S GHIORSE
D GRANVILLE
D HOPKINS
C HOPPEL
D HENRY
R KASTE
M KLUSEWITZ
M LEADORE
R LIEB
E RIGAS
J SANDS
D SPAGNUOLO
W SPURGEON
J TZENG

NO. OF
COPIES ORGANIZATION

ABERDEEN PROVING GROUND (CONT)

E WETZEL
A FRYDMAN
AMRSL WM MC
J BEATTY
E CHIN
J MONTGOMERY
A WERECZCAK
J LASALVIA
J WELLS
AMSRL WM MD
W ROY
S WALSH
AMSRL WM T
B BURNS
M ZOLTOSKI
AMSRL WM TA
W GILLICH
T HAVEL
J RUNYEON
M BURKINS
E HORWATH
B GOOCH
W BRUCHEY
M NORMANDIA
AMRSL WM TB
D KOOKER
P BAKER
AMSRL WM TC
R COATES
AMSRL WM TD
A DAS GUPTA
T HADUCH
T MOYNIHAN
F GREGORY
M RAFTENBERG
M BOTELER
T WEERASOORIYA
D DANDEKAR
A DIETRICH
AMSRL WM TE
A NIILER
J POWELL
AMSRL SS SD
H WALLACE
AMSRL SS SE DS
R REYZER
R ATKINSON

NO. OF COPIES	ORGANIZATION
1	LTD R MARTIN MERL TAMWORTH RD HERTFORD SG13 7DG UK
1	SMC SCOTLAND P W LAY DERA ROSYTH ROSYTH ROYAL DOCKYARD DUNFERMLINE FIFE KY 11 2XR UK
1	CIVIL AVIATION ADMINSTRATION T GOTTESMAN PO BOX 8 BEN GURION INTERNL AIRPORT LOD 70150 ISRAEL
1	AEROSPATIALE S ANDRE A BTE CC RTE MD132 316 ROUTE DE BAYONNE TOULOUSE 31060 FRANCE
1	DRA FORT HALSTEAD P N JONES SEVEN OAKS KENT TN 147BP UK
1	DEFENSE RESEARCH ESTAB VALCARTIER F LESAGE COURCELETTE QUEBEC COA IRO CANADA
1	SWISS FEDERAL ARMAMENTS WKS W LANZ ALLMENDSTRASSE 86 3602 THUN SWITZERLAND
1	DYNAMEC RESEARCH AB AKE PERSSON BOX 201 SE 151 23 SODERTALJE SWEDEN

NO. OF COPIES	ORGANIZATION
1	ISRAEL INST OF TECHNOLOGY S BODNER FACULTY OF MECHANICAL ENGR HAIFA 3200 ISRAEL
1	DSTO AMRL WEAPONS SYSTEMS DIVISION N BURMAN RLLWS SALISBURY SOUTH AUSTRALIA 5108 AUSTRALIA
1	ECOLE ROYAL MILITAIRE E CELENS AVE DE LA RENAISSANCE 30 1040 BRUXELLE BELGIQUE
1	DEF RES ESTABLISHMENT VALCARTIER A DUPUIS 2459 BOULEVARD PIE XI NORTH VALCARTIER QUEBEC CANADA PO BOX 8800 COURCELETTE GOA IRO QUEBEC CANADA
1	INSTITUT FRANCO ALLEMAND DE RECHERCHES DE SAINT LOUIS DE M GIRAUD 5 RUE DU GENERAL CASSAGNOU BOITE POSTALE 34 F 68301 SAINT LOUIS CEDEX FRANCE
1	ECOLE POLYTECH J MANSON DMX LTC CH 1015 LAUSANNE SWITZERLAND

NO. OF COPIES	ORGANIZATION
1	TNO PRINS MAURITS LABORATORY R IJSSELSTEIN LANGE KLEIWEG 137 PO BOX 45 2280 AA RIJSWIJK THE NETHERLANDS
2	FOA NATL DEFENSE RESEARCH ESTAB DIR DEPT OF WEAPONS & PROTECTION B JANZON R HOLMLIN S 172 90 STOCKHOLM SWEDEN
2	DEFENSE TECH & PROC AGENCY GROUND I CREWTHER GENERAL HERZOG HAUS 3602 THUN SWITZERLAND
1	MINISTRY OF DEFENCE RAFAEL ARMAMENT DEVELOPMENT AUTH M MAYSELESS PO BOX 2250 HAIFA 31021 ISRAEL
1	TNO DEFENSE RESEARCH I H PASMAN POSTBUS 6006 2600 JA DELFT THE NETHERLANDS
1	B HIRSCH TACHKEMONY ST 6 NETAMUA 42611 ISRAEL
1	DEUTSCHE AEROSPACE AG DYNAMICS SYSTEMS M HELD PO BOX 1340 D 86523 SCHROBENHAUSEN GERMANY

REPORT DOCUMENTATION PAGE

Form Approved
OMB No. 0704-0188

1. AGENCY USE ONLY *(Leave blank)*	2. REPORT DATE	3. REPORT TYPE AND DATES COVERED
	November 2001	Final, September 1999-October 2000

4. TITLE AND SUBTITLE
Electron Beam (E-Beam) Processing as a Means of Achieving High Performance Composite Structures

5. FUNDING NUMBERS
PP1109

6. AUTHOR(S)
James M. Sands, Steven H. McKnight, Bruce K. Fink, Anna Yen,* and Giuseppe R. Palmese†

7. PERFORMING ORGANIZATION NAME(S) AND ADDRESS(ES)
U.S. Army Research Laboratory
ATTN: AMSRL-WM-MB
Aberdeen Proving Ground, MD 21005-5069

8. PERFORMING ORGANIZATION REPORT NUMBER
ARL-TR-2613

9. SPONSORING/MONITORING AGENCY NAMES(S) AND ADDRESS(ES)
Strategic Environmental Research and Development Program
901 North Stuart Street, Suite 303
Arlington, VA 22203

10.SPONSORING/MONITORING AGENCY REPORT NUMBER

11. SUPPLEMENTARY NOTES
* Northrop Grumman Corporation, 1 Hornet Way, El Segundo, CA 90245.
† Drexel University, 3141 Chestnut Street, Philadelphia, PA 19104.

12a. DISTRIBUTION/AVAILABILITY STATEMENT
Approved for public release; distribution is unlimited.

12b. DISTRIBUTION CODE

13. ABSTRACT *(Maximum 200 words)*

Electron-beam (E-beam) curing is among the key out-of-autoclave technologies being explored for future advanced composite and adhesive applications. E-beam irradiation curing is capable of rapid and through-thickness curing of composite samples up to 2-in thickness, eliminating the need for long cure cycles in the autoclave. However, current resin and adhesive chemistries are optimized for cure by thermal initiation, which involves slow ramps and long cure cycles, particularly for thermoset composites based on epoxides. Therefore, in order to provide improved performance in composite systems cured by E-beam irradiation, a program was undertaken to investigate performance and formulation effects in two E-beam curable systems. One system, a free-radical-cured acrylic system, introduces the concept of interpentrating network structures as a means of meeting performance requirements in E-beam-processed composites. The second resin system incorporates cationic curing of epoxides induced through Lewis acid or cation generating initiators. Additionally, a new approach to toughened interpenetrating polymer networks (IPNs) based on simultaneous cure using both free-radical and cationic-cure mechanisms is proposed along with initial experimental characterizations. The results of formulation and processing modifications on key properties of adhesives, resins, and composites structures are demonstrated.

14. SUBJECT TERMS	15. NUMBER OF PAGES
electron beam, irradiation cure, composites, epoxide, IPN, polymer network, adhesives	74
	16. PRICE CODE

17. SECURITY CLASSIFICATION OF REPORT	18. SECURITY CLASSIFICATION OF THIS PAGE	19. SECURITY CLASSIFICATION OF ABSTRACT	20. LIMITATION OF ABSTRACT
UNCLASSIFIED	UNCLASSIFIED	UNCLASSIFIED	UL

INTENTIONALLY LEFT BLANK.